Chlorine Deactivation in the Lower Stratospheric Polar Regions During Late Winter: Results from UARS

M. L. Santee, L. Froidevaux, G. L. Manney, W. G. Read, and J. W. Waters
Jet Propulsion Laboratory, California Institute of Technology, Pasadena

M. P. Chipperfield
Department of Chemistry, University of Cambridge, UK

A. E. Roche, J. B. Kumer and J. L. Mergenthaler
Lockheed Palo Alto Research Laboratory, Palo Alto, California

J. M. Russell III
NASA Langley Research Center, Hampton, Virginia

Received _____; accepted _____

Short title: CHLORINE DEACTIVATION FROM UARS DATA

Abstract. The recovery of the perturbed chlorine chemistry in the lower stratospheric polar regions of both hemispheres is investigated using recent data from the Upper Atmosphere Research Satellite (UARS). Microwave Limb Sounder (MLS) measurements of ClO within the polar vortices are correlated with both simultaneous Cryogenic Limb Array Etalon Spectrometer (CLAES) measurements of $ClONO_2$ and Halogen Occultation Experiment (HALOE) measurements of HCl obtained shortly after the MLS and CLAES data. Time series of vortex-averaged mixing ratios are calculated on two potential temperature surfaces (585 K and 465 K) in the lower stratosphere for approximately month-long intervals during late winter in each hemisphere. The observed mixing ratios are adjusted for the effects of vertical transport using diabatic vertical velocities estimated from CLAES tracer data. In the northern hemisphere, the decrease in ClO is balanced on both surfaces by an increase in $ClONO_2$. In the southern hemisphere, continuing polar stratospheric cloud activity prevents ClO from undergoing sustained decline until the latter half of the study period. In contrast to the northern hemisphere, there is no significant chemical change in $ClONO_2$ at 465 K, and there is an apparent decrease in $ClONO_2$ at 585 K, even after the enhanced ClO abundances have started to recede. Results from an isentropic three-dimensional chemical transport model initialized with UARS data and run with $OH + ClO \rightarrow HCl + O_2$ as an 8% channel suggest that the primary recovery product in the south during this time period is not $ClONO_2$, but HCl. HALOE HCl mixing ratios are linearly extrapolated back to the time of the MLS and CLAES data. At 585 K, the chlorine budget can be made to balance by extrapolating back to a value of 0.5 ppbv for the HCl at the beginning of the study period. At 465 K, the contribution from extrapolated HCl is not sufficient to offset the observed loss in ClO, and there is a slight imbalance between the decrease in the reactive chlorine and the change in the chlorine reservoirs. The difficulty in closing the chlorine budget in the southern hemisphere may arise from complications caused by ongoing activation, incomplete photochemical assumptions, or inadequate data quality.

Introduction

Chlorine chemistry is now known to be responsible for the severe depletion in lower stratospheric ozone observed during late winter and early spring over Antarctica [see, e.g., *Solomon*, 1988, 1990; *McElroy and Salawitch*, 1989; *Anderson et al.*, 1991; *Brune et al.*, 1991]. Observed decreases in Arctic lower stratospheric ozone have also been shown to be consistent with chlorine catalyzed destruction [e.g., *Salawitch et al.*, 1990, 1993; *Schoeberl et al.*, 1990; *Manney et al.*, 1994*a*; *Traub et al.*, 1994]. Reactive chlorine is produced through heterogeneous processes occurring on the surfaces of polar stratospheric clouds (PSCs), which form in the low temperatures of polar winter. These heterogeneous reactions rapidly convert the reservoir species HCl and $ClONO_2$, where most of the inorganic chlorine in the lower stratosphere resides under nonperturbed conditions [*Webster et al.*, 1993], to species such as Cl_2 and HOCl that are easily photolyzed. Following exposure of the processed air to sunlight, the dominant daytime chlorine species is ClO. Maintenance of high ClO levels leads to ozone loss through a catalytic cycle involving ClO dimer (Cl_2O_2) formation [*Molina and Molina*, 1987].

The timescale for recovery of the perturbed chlorine chemistry in the lower stratosphere is an important topic because the rate at which enhanced ClO abundances recede bears directly on the cumulative ozone loss at high latitudes. One pathway by which reactive chlorine is shifted back to reservoir form is $ClO + NO_2 + M \rightarrow ClONO_2 + M$. In addition to promoting chlorine repartitioning, heterogeneous processes also inhibit reformation of $ClONO_2$ by sequestering reactive nitrogen as HNO_3 in PSC particles. When temperatures rise above the PSC evaporation threshold, gaseous HNO_3 is released; the HNO_3 then photolyzes (on a timescale of ~30 days for a solar zenith angle of 70° [*Kawa et al.*, 1992]) to produce NO_2. If sufficient NO_2 is available, $ClONO_2$ formation takes place in a few hours. Alternatively, chlorine deactivation can proceed via the reaction $Cl + CH_4 \rightarrow HCl + CH_3$. Under non-ozone-depleted conditions, the timescale for HCl reformation is roughly comparable to the timescale for HNO_3 photolysis [*Kawa et al.*, 1992].

However, [*Prather et al.*, 1990] and *Cicerone and Jaffe* [1990] have shown that very low ozone concentrations lead to a highly nonlinear chemical system in which the conversion of ClO to HCl is substantially accelerated through an increase in the Cl to ClO abundance ratio. This conversion to HCl under low-ozone conditions has been observed in UARS data by *Douglass et al.* [1995].

Significant interhemispheric differences in the recovery timescale are expected due to underlying differences in seasonal temperature patterns and vortex behavior [see, e.g., *Anderson et al.*, 1989; *WMO 1991 Report*]. On average, temperatures in the Arctic vortex are ~15–20 K higher than in the Antarctic, and the Arctic vortex is much less stable, leading to fewer and less persistent PSC events in the Arctic. Denitrification the removal of nitrogen from the lower stratosphere through gravitational settling of PSC particles containing HNO_3 is much less extensive in the Arctic than in the Antarctic [cf. *Fahey et al.*, 1989; *Toon et al.*, 1989; *Coffey et al.*, 1989; *Mankin et al.*, 1990; *Kawa et al.*, 1990; *Poole and Pitts*, 1994; *Santee et al.*, 1995]. Although enhanced ClO abundances have been observed in the polar vortices of both hemispheres [*de Zafra et al.*, 1987; *Anderson et al.*, 1989; *Waters et al.*, 1993*a,b*], the accompanying loss of Arctic ozone has been much less severe [*Manney et al.*, 1994a] than that over Antarctica. The warmer temperatures, greater dynamical activity, and continued presence of HNO_3 throughout northern winter moderate ozone loss and prevent the formation of an Arctic ozone "hole" [*Brune et al.*, 1991; *Schoeberl and Hartmann*, 1991; *Santee et al.*, 1995]. Differences in the late winter/early spring HNO_3 and O_3 concentrations between the two hemispheres lead to dissimilarities in the production rates of the chlorine reservoirs.

Chlorine deactivation has been the subject of several previous investigations. *Toohey et al.* [1993] and *Webster et al.* [1993] report simultaneous *in situ* measurements of ClO and HCl from the second Airborne Arctic Stratospheric Expedition (AASE II) in the 1991–1992 Arctic winter. They find that decreasing ClO abundances during the recovery phase are consistent with the rapid formation of $ClONO_2$ (calculated from an estimate of

the total available inorganic chlorine), while HCl remains substantially depleted through the end of the observational period in February 1992. Contemporaneous observational [*Adrian et al.*, 1994; *Oelhaf et al.*, 1994; *Bell et al.*, 1994] and modeling [*Lutman et al.*, 1994; *Müller et al.*, 1994] studies from the European Arctic Stratospheric Ozone Experiment (EASOE) find the same recovery pattern: after cessation of PSC activity, there is an almost complete conversion of active chlorine to $ClONO_2$, which remains the dominant inorganic chlorine compound for more than a month. These recent findings confirm the conclusions from earlier modeling studies constrained by AASE observations [*Jones et al.*, 1990; *McKenna et al.*, 1990]. In Antarctica, infrared solar spectra recorded at McMurdo in late winter/early spring 1986 indicate a twofold increase in column HCl + $ClONO_2$ associated with rapidly rising temperatures [*Farmer et al.*, 1987]. While the sum of HCl and $ClONO_2$ remains roughly constant thereafter, the $ClONO_2$/HCl ratio gradually declines from 1.5 in late September to 0.3 in late October. *Liu et al.* [1992] also use HCl column amounts retrieved from infrared solar spectra obtained at McMurdo, in combination with a one dimensional photochemical model, to show that almost all active chlorine species are converted back to HCl by mid- October. Rapid conversion of ClO to the reservoirs $ClONO_2$ and HCl occurs once PSCs evaporate, followed by slow repartitioning between the reservoirs. *Schoeberl et al.* [1993] perform trajectory analyses of ClO and NO measurements from both Arctic and Antarctic aircraft campaigns and conclude that production of $ClONO_2$ is the main mechanism for the initial decay of high ClO concentrations when the air is not denitrified; in highly denitrified parcels, lack of HNO_3 (and therefore NO_2) prevents transformation of ClO to $ClONO_2$, and ClO remains enhanced.

In this paper, we use recent data from the Upper Atmosphere Research Satellite (UARS) to examine chlorine reservoir recovery in the lower stratospheric polar regions of both hemispheres. Microwave Limb Sounder (MLS) measurements of ClO within the polar vortices are correlated with both simultaneous Cryogenic Limb Array Etalon

Spectrometer (CLAES) observations of $ClONO_2$ and Halogen Occultation Experiment (HALOE) observations of HCl obtained shortly after the MLS and CLAES data. We analyze time series of vortex-averaged mixing ratios on two potential temperature surfaces (585 K and 465 K) in the lower stratosphere for approximately month-long intervals during late winter: August 17 - September 17, 1992 in the southern hemisphere and February 12 March 16, 1993 in the northern hemisphere. We focus on the late winter balance between the decay of reactive chlorine and the growth of chlorine reservoir species based on these data sets, and we compare the observations results with those from a three-dimensional chemical transport model [see the companion paper by *Chipperfield et al.*, 1995] initialized with UARS data.

Data and Instrument Description

MLS acquires stratospheric measurements of millimeter-wavelength thermal emission that are not degraded by PSCs or aerosol. The measurement technique and the instrument are described in detail by *Waters* [1993] and *Barath et al.* [1993], respectively. MLS observations of ClO have been presented previously by *Waters et al.* [1993*a*,*b*; 1995*a*] and *Manney et al.* [1994*a*]. The estimated precision (rms) and absolute accuracy of an individual ClO profile in the lower stratosphere are ~0.5 ppbv (parts per 10^9 by volume) and 15-20%, respectively [*Waters et al.*, 1995*b*] for Version 3 files. In this study, we utilize ClO values from preliminary algorithms that also retrieve HNO_3, eliminating a bias error in the Version 3 ClO data [*Waters et al.*, 1995*b*]. These ClO data have an accuracy of about 10%.

CLAES [*Roche et al.*, 1993*a*] measures infrared thermal emission in nine spectral regions between 3.5 μm and 13 μm. MLS and CLAES observations are essentially simultaneous and co-located (typically to within a few tens of kilometers). CLAES $ClONO_2$ measurements have been reported by *Roche et al.* [1993*b*; 1994]; here we use Version 7 files, which have an estimated systematic error of less than 20% and a single-profile pre-

cision of ~0.2 ppbv in the lower stratosphere [*Mergenthaler et al.*, 1995]. To eliminate spikes and other known artifacts in the data, all points for which the $ClONO_2$ value either exceeds 3.5 ppbv or exceeds 1.5 ppbv with an associated error of greater than 50% are excluded from the analysis [*Mergenthaler et al.*, 1995]. We also utilize CLAES observations of the dynamical tracers CH_4 and N_2O [*Kumer et al.*, 1993; *Roche et al.*, 1995]. For CH_4, the estimated systematic error and precision are about 15% and 0.1 ppmv, respectively, at 46 hPa, and the mixing ratios are most reliable for values below 1.5 ppmv. For N_2O, the estimated systematic error and precision are about 20% and 20 ppbv, respectively, at 46 hPa, and the mixing ratios are most reliable for values below 250 ppbv. In addition to constituent mixing ratios, aerosol extinction coefficients are also retrieved from the measured spectra [*Mergenthaler et al.*, 1993; *Massie et al.*, 1995]. The aerosol data we show here are from the 790 cm^{-1} spectral region, where there is strong spectral contrast between gas (O_3 and CO_2) line emission and aerosol continuum emission.

Both CLAES and MLS are situated on the anti-sun side of the spacecraft, and both of their optical pointing axes are directed approximately 23° down from the local horizontal at the observation point. This pointing geometry, coupled with the 57° inclination of the UARS orbit, leads to measurement coverage from 80° latitude on one side of the equator to 34° on the other. The UARS orbit plane precesses in such a way that all local solar times are sampled in about 36 days (getting ~20 min earlier each day at a given latitude), after which the spacecraft is rotated 180° about its yaw axis. Thus, 10 times per year MLS and CLAES alternate between viewing northern and southern high latitudes.

HALOE uses solar occultation to measure the attenuation of infrared solar energy due to stratospheric constituents [*Russell et al.*, 1993]. In this study, we use Version 16 HCl data, which are described by *Russell et al.* [1995]. Because measurements are made only at the spacecraft sunrise and sunset times, daily sampling typically consists of 15 sunrise profiles at one particular latitude, and 15 sunset profiles in the opposite

hemisphere. The 11 ALOE observing pattern moves slowly north and south throughout the year, with wintertime coverage of the most extreme southern latitudes (nearly to 80°S) occurring from mid-September through mid-October, and wintertime coverage of the most extreme northern latitudes (nearly to SOON) occurring from mid-March through mid-April. In the 1992 southern and 1992-93 northern late winter periods, HALOE measurements are not obtained within the polar vortices until after the spacecraft has yawed towards the opposite hemisphere; thus, the HALOE high-latitude data are not coincident with either the MLS or CLAES data.

1992 Southern Hemisphere Winter

Behavior of ClO and $ClONO_2$

As discussed in the Introduction, high levels of ClO in the vortex follow from the heterogeneous activation of chlorine as temperatures fall below the PSC formation threshold (~195 K [*Turco et al.*, 1989]) in early winter. Elevated levels (mixing ratios greater than 1 ppbv) of lower stratospheric ClO were observed in portions of the southern polar vortex as early as 2 June (the beginning of an MLS south-viewing period) [*Waters et al.*, 1993*a*,*b*]. ClO abundances continued to increase throughout the winter, and at the start of the next south-viewing period on 17 August 1992, MLS measured lower stratospheric ClO values of more than 2 ppbv in most of the sunlit area poleward of 60°S [*Waters et al.*, 1993*a*,*b*]. It is for this late winter (17 August - 17 September, 1992) yaw period that we will examine the relationship between the decrease in ClO and the increase in the reservoir species $ClONO_2$ and HCl.

The behavior of MLS ClO on three selected days at the beginning, middle, and end of the southern hemisphere late winter yaw period is shown in Figure 1*a*. The data have been interpolated onto constant potential temperature (Θ) surfaces at 585 K (corresponding to ~24 km, 20 hPa for the cold temperatures characteristic of the polar

vortex) and 465 K (~19 km, 50 hPa) using United States National Meteorological Center (NMC) temperatures. Only data from the "day" side of the orbit are shown because ClO abundances drop sharply in regions where the solar zenith angle (Figure 1*b*) is greater than ~94°, due to lack of Cl_2O_2 photolysis. Superimposed on each of the maps are three contours of potential vorticity (PV), calculated from NMC temperatures and derived winds using the algorithm described by *Manney and Zurek* [1993]. These PV contours are used to delimit different areas over which averaged mixing ratios are calculated. The outermost contour represents a typical definition of the vortex edge during winter [e.g., *Manney et al.*, 1993] and coincides with a strong barrier to mixing [*Manney et al.*, 1994*b*]. The innermost contour on each Θ surface has a PV value twice that of the outermost one. The intermediate contour is situated poleward of the vortex boundary, and using it reduces the potential impact of horizontal transport from lower latitudes on the averaged mixing ratios. It more closely delineates the region of high ClO at 465 K in mid-August, and it also closely approximates the edge of the region of low values of N_2O and CH_4 (not shown) caused by stronger diabatic descent within the vortex. The PV contours indicate that the vortex is approximately symmetric with respect to the pole throughout this period, and its size, shape, and strength are roughly constant at both levels.

From mid-August to mid-September, the outside edge of enhanced ClO retreats poleward. Elevated ClO abundances recede more rapidly at 585 K than at 465 K, with the majority of the decrease occurring in the latter half of the period. The area poleward of 52°S in which daytime ClO mixing ratios exceed 1 ppbv, shown in Figure 2, is a diagnostic of the time and altitude dependence of the decay of activated chlorine. The value of 52° is selected to generally encompass the maximum areal extent of the vortex at these levels during this time period while excluding lower latitudes (where ClO is not enhanced). The lower stratospheric minimum values occurring at the beginning of September are artifacts caused by a brief interval in the middle of the yaw period during which there are essentially no daylight measurements due to precession of the orbit. The

slope and spacing of the contours in Figure 2 illustrate the more rapid decline in ClO at the higher Θ levels, and that this decline intensifies at the beginning of September.

In the southern polar region, PSCs typically persist at 18 km until at least mid- to late September [*McCormick et al.*, 1989; *Poole and Pitts*, 1994]. In 1987, PSCs were present at this level into mid-October [*McCormick et al.*, 1989; *Poole and Pitts*, 1994], and results from ER-2 aircraft flights between 23 August and 22 September 1987 show that ClO mixing ratios at 18 km increased throughout this period [*Brune et al.*, 1989]. *Jones et al.* [1989] use the ER-2 observations from early September 1987 to initialize a photochemical model integrated along air parcel trajectories, and find that maintenance of elevated ClO concentrations is very dependent on the frequency and duration of PSC events. In this study, we use CLAES measurements of aerosol extinction to assess the possibility of continued chlorine activation during our observational period. The area in which aerosol extinction coefficients in the region poleward of 52°S exceed 1.0×10^{-3} km^{-1} [*Turco et al.*, 1989] is given in Figure 3. At the beginning of the late winter yaw period in mid-August, PSC activity is as extensive as it was during the previous June-July south-looking interval (not shown), and heterogeneous chlorine activation is expected to be ongoing. Maps of aerosol extinction on individual days (also not shown) indicate that, although there are no significant PSC events observed to extend up to the 585 K level after the first few days of September, there continue to be intermittent localized PSC events at 465 K as late as 15 September. These episodic PSCs may partially explain the slower decline in ClO at 465 K than at 585 K. Because the focus here is on the *deactivation* of chlorine, we will limit the study to the latter half of the yaw period (starting on 3 September), when PSC activity is beginning to subside and (as seen in Figure 2) the high ClO abundances are receding.

If the primary reservoir for chlorine during the initial stages of recovery were $ClONO_2$, then production of $ClONO_2$ would parallel the reduction in ClO evident in Figures 1 and 2. Maps of CLAES $ClONO_2$ during the late winter interval are shown in Figure 4. To

ensure that the same air parcels are being considered for both ClO and $ClONO_2$, these maps are also constructed using data from the "day" side of the orbit only. As discussed by *Roche et al.* [1 9936; 1994], $ClONO_2$ mixing ratios rise steeply from mid-latitudes to form a roughly circumpolar collar of enhanced abundances, with some intrusion of high $ClONO_2$ iuto the vortex core, where values are generally much smaller than in the collar region. By mid-September, the high values of the collar region have diminished at both Θ levels, and an overall increase in $ClONO_2$ comparable to the decrease in ClO is uot seen. As shown in Figure 5, the area poleward of 52° S distinguished by high $ClONO_2$ abundances (> 1.5 ppbv) is essentially constant at 465 K but decreases at 585 K throughout the yaw period.

Effects of Vertical Transport

One of the issues that must be addressed in contrasting the behavior of ClO and $ClONO_2$ is the possible effect of vertical transport on the mixing ratios at these levels. As the polar regions fall into darkness after the autumnal equinox, radiative processes rapidly cool the polar stratosphere, the vortex spins up, and strong downward motion over this area begins [*Schoeberl and Hartmann*, 1991]. The descending air carries with it the chemical composition of the upper stratosphere, and therefore, depending on the vertical profile of a given species, can produce steep horizontal gradients in its concentration on isentropic surfaces. Both N_2O and CH_4 have long chemical lifetimes with tropospheric sources and stratospheric sinks, and have been shown to be useful as conservative tracers of stratospheric air motions [*Loewenstein et al.*, 1989, 1990; *Collins et al.*, 1993].

We estimate the vertical velocities at 585 K and 465 K from CLAES measurements of N_2O and CH_4. Vortex-averaged mixing ratios are calculated by dividing the area integral of the mixing ratio inside a *PV* contour by the area enclosed by that contour. This calculation is performed for the three *PV* contours shown in Figure 1*a*. Similar results are obtained for all PV values; here we discuss the results from the intermediate

contour only. Daily vortex- averaged mixing ratios for both N_2O and CH_4 are shown in Figure 6 as a function of time. For perfect tracers in the absence of diabatic descent, the lines fit to the averaged mixing ratios would have zero slope. Under the assumption that the trends exhibited by these species arise solely from diabatic descent, the slopes of these lines are used in the tracer continuity equation to estimate average vertical velocities., The vertical velocities estimated from the two tracers are generally consistent, and are averaged together to obtain the overall estimate of tile vertical velocity at each (-) level. Uncertainties are assigned by propagating into the velocity calculation the uncertainties in the slopes of the lines fit to the daily vortex- averaged mixing ratios and the standard deviations of the tracer vertical profiles, and then augmenting the resulting error if necessary to ensure that the overall average encompasses the estimates from both tracers. This is a deliberately conservative process intended to provide an upper limit on the uncertainty estimate.

Based 011 this approach, we find the vortex-averaged descent rate to be 0.5±0.3 111111/s at 585 K and 0.7 ± 0.'2 mm/s at 465 1{ when only the latter half of the yaw period is considered (velocities are higher when trends are taken over the entire yaw period, particularly at 585 K). It should be noted that these are vortex-averaged values; locally, velocities could depart significantly from the vortex averages. Within the uncertainties, these values are in agreement with estimates of the lower stratospheric vertical velocity (1.() mm/s) in August 1992 obtained from simulated air parcel trajectories by *Manney et al.* [1 994 6]. They also agree very well with the average lower stratospheric descent rates (1.5- 1.8 km/month, or 0.6- ().7 mm/s) estimated for tile 1992 winter season from UARS HALOE CH_4 trends [*Schoeberl et* d., 1995]. However, they are larger than the late winter residual vertical velocities diagnosed from 1987 NM(; temperatures and Airborne Antarctic Ozone Experiment (AAOE) 11_20 and O_3 data by *Schoeberl et al.* [1 992], which range from 0.1 to 0.2 111111/s between 18 and 22 km at 70°S. More recent radiative transfer calculations by *Rosenfield et al. [1* 994], based 011 NMC temperatures during both the

1987 and 1992 Antarctic winter seasons, also produce smaller average diabatic descent rates in the lower stratospheric vortex (~0.4–0.9 km/month, or ~0.2–0.3 mm/s) than those estimated here from the CLAES tracer data. It is important to note, however, that the rates deduced by *Rosenfield et al.* [1994] represent an average computed from the descent of air over an eight-month period from March through October, and a direct comparison with our late-winter velocity estimates is an oversimplification.

Once the descent rate at each level has been estimated, the changes in ClO and $ClONO_2$ due to vertical transport can also be calculated from the tracer continuity equation, assuming constant velocities throughout the two-week interval. This calculation would not be necessary for species that are short-lived compared to a two-week interval, because local photochemical conditions -- not dynamics -- drive changes in their abundances. However, total reactive chlorine ClO_x ($ClO_x = ClO + 2Cl_2O_2$) is affected by dynamics, and it in turn affects ClO and $ClONO_2$. As discussed further below, the approximate nature of the approach used here to account for the effects of dynamics is not a major factor in the overall conclusions. The impact of diabatic descent on the mixing ratios of a constituent depends not only on the magnitude of the vertical velocity but also on the shape of the constituent's vertical profile. The ClO mixing ratio profile (Figure 7*a*) drops sharply above 465 K, and the downward transport of air with lower ClO abundances accounts for a portion of the observed decline in ClO values at both 585 K and 465 K. Because the peak of the $ClONO_2$ profile (Figure 7*b*) occurs near 585 K, descent is estimated to produce a decrease in $ClONO_2$ concentrations at that level, but an increase in $ClONO_2$ concentrations at 465 K. Figure 8 shows daily vortex averages of the observed ClO and $ClONO_2$ abundances, along with adjusted values obtained by subtracting the estimated changes in mixing ratio due to diabatic descent. These adjusted mixing ratio values reflect the trends in the species that can be attributed to chemical processes. The results presented in Figure 8 are based on averages within the intermediate *PV* contour in Figure 1*a*, restricted to the latter half of the yaw period (after 3 September).

Similar behavior is found for vortex averages within the other two PV contours. For this period, the implied chemical loss in ClO is approximately 0.4 ± 0.1 ppbv at 585 K and 0.3 ± 0.1 ppbv at 465 K, based on linear fits to the daily averages. Although there is a clear decreasing trend in ClO throughout this interval at both levels, there is an apparent *decrease* of 0.1 ± 0.1 ppbv in the adjusted $ClONO_2$ mixing ratios at 585 K, and there is no significant chemical change in $ClONO_2$ at 465 K (-0.0 ± 0.1 ppbv). No increase in $ClONO_2$ is found to offset the decrease in ClO even when the values at the extreme limits of the uncertainties are used. These adjusted ClO and $ClONO_2$ concentrations are computed using the nominal magnitudes of the vertical velocities; however, calculations over the range of velocity values defined by the uncertainties yield very similar results. In fact, sensitivity tests indicate that for there to be an increase in $ClONO_2$ balancing the decrease in ClO there would have to be very strong descent ($\sim$2.3 mm/s) at 585 K but ascent ($\sim$0.7 mm/s) at 465 K.

To ensure that a consistent set of air parcels is being evaluated for all species, in the preceding calculations all vortex averages include data from the "day" side of the orbit only. However, if any of the chlorine released from ClO is being converted into $ClONO_2$, then $ClONO_2$ mixing ratios at night could be slightly larger than those during the day, when $ClONO_2$ is subject to photodissociation. We therefore examine vortex averages of $ClONO_2$ mixing ratios from the "night" side of the orbit, adjusted using the diabatic vertical velocities calculated above. In this case there is no change (-0.0 ± 0.1 ppbv) at 585 K, and a decrease of 0.1 ± 0.1 ppbv at 465 K. As before, no increase in $ClONO_2$ is found to offset the decrease in ClO even when the values at the extreme limits of the uncertainties are used.

Results from the Chemical Transport Model

We also use the SLIMCAT isentropic three-dimensional chemical transport model [see the companion paper by *Chipperfield et al.*, 1995] to investigate the decay of enhanced

1987 and 1992 Antarctic winter seasons, also produce smaller average diabatic descent rates in the lower stratospheric vortex ($\sim$0.4–0.9 km/month, or $\sim$0.2–0.3 mm/s) than those estimated here from the CLAES tracer data. It is important to note, however, that the rates deduced by *Rosenfield et al.* [1994] represent an average computed from the descent of air over an eight-month period from March through October, and a direct comparison with our late-winter velocity estimates is an oversimplification.

Once the descent rate at each level has been estimated, the changes in ClO and $ClONO_2$ due to vertical transport can also be calculated from the tracer continuity equation, assuming constant velocities throughout the two-week interval. This calculation would not be necessary for species that are short-lived compared to a two-week interval, because local photochemical conditions -- not dynamics – drive changes in their abundances. However, total reactive chlorine ClO_x (ClO_x = ClO + $2Cl_2O_2$) is affected by dynamics, and it in turn affects ClO and $ClONO_2$. As discussed further below, the approximate nature of the approach used here to account for the effects of dynamics is not a major factor in the overall conclusions. The impact of diabatic descent on the mixing ratios of a constituent depends not only on the magnitude of the vertical velocity but also on the shape of the constituent's vertical profile. The ClO mixing ratio profile (Figure 7*a*) drops sharply above 465 K, and the downward transport of air with lower ClO abundances accounts for a portion of the observed decline in ClO values at both 585 K and 465 K. Because the peak of the $ClONO_2$ profile (Figure 7*b*) occurs near 585 K, descent is estimated to produce a decrease in $ClONO_2$ concentrations at that level, but an increase in $ClONO_2$ concentrations at 465 K. Figure 8 shows daily vortex averages of the observed ClO and $ClONO_2$ abundances, along with adjusted values obtained by subtracting the estimated changes in mixing ratio due to diabatic descent. These adjusted mixing ratio values reflect the trends in the species that can be attributed to chemical processes. The results presented in Figure 8 are based on averages within the intermediate *PV* contour in Figure 1*a*, restricted to the latter half of the yaw period (after 3 September).

ClO in the Antarctic vortex. ECMWF meteorological analyses are used to specify the horizontal winds and temperatures with a spectral truncation of T42, yielding a model horizontal resolution of 2.8° x 2.8°. The model employs a detailed stratospheric chemistry scheme with treatment of heterogeneous reactions on PSCs and sulfate aerosols. It is initialized with UARS data for 31 August 1992 interpolated onto the '1'42 Gaussian grid and is run on both the 585 K and 465 K surfaces. In the companion paper, *Chipperfield et* al. [1995] report on results from the basic model as well as those from several sensitivity tests; here we present results only from run I) of the companion paper. This run treats 465 K and 585 K as separate unconnected isentropic surfaces with no vertical transport between them. It also includes the reaction $OH + ClO \rightarrow HCl + O_2$ as an 8% channel. This pathway has been shown to improve the agreement, between photochemical models and observations of ClO, HCl and 03 in the upper stratosphere [*McElroy and Salawitch*, 1989; *Natarajan and Callis*, 1991; *Chandra et al.,* 1993; *Toumi and Bekki*, 1993; *Minschwaner et al.,* 1993]. *Chipperfield et al.* [199(5] show that the inclusion of this channel is also important in the lower stIal,c~sl}ll['if:, affecting model results at both 585 K and 465 K.

Vortex averages of mode] chlorine species from this run are shown in Figure 9, along with MI, S ClO and CLAES $ClONO_2$ data. The model fields are sampled at 1200UT except for ClO and $ClONO_2$, which are sampled at the same local time as the MLS and CLAES measureme nts. Total inorganic chlorine (ClO_y) is essentially constant at 3.0 ppbv at 585 K and 2.8 ppbv at 465 K. The model reproduc es the M LS ClO abundances and downward trend at 585 K, but at 465 K it underestimates MLS (lO by up to 0.4 ppbv (see *Chipperfield et al.* [1995] f o r an elaboration of t he low model ClO). A t 465 K it also indicates a slightly increasing trend in ClO (not seen in the data) which is probably related to the fact that the model overestimates the extent of the ongoing PSC processing. Similarly, the model reproduces the CLAES $ClONO_2$ data fairly well at 585 K (although it indicates a small increase in $ClONO_2$ over the interval which is not seen in the data), but at 465 K it underestimates CLAES ($lONO_2$ by as much as 0.6 ppbv. As discussed

by *Chipperfield et al.* [1995], inclusion of the $OH + ClO \rightarrow HCl + O_2$ reaction suppresses the increase in $ClONO_2$ and promotes the conversion of ClO to HCl. The calculated changes in $ClONO_2$ and HOCl are not significant, and the main recovery is predicted to be into HCl at both 585 K and 465 K.

For the calculations presented in Figure 8 we have neglected the effects of the dimer, Cl_2O_2, produced from ClO recombination: $ClO + ClO + M \rightarrow Cl_2O_2 + M$. Since there are no measurements of Cl_2O_2, its contribution is assessed from model results. The simulations show a more rapid decay in ClO_x than in ClO, particularly at 585 K (Figure 9). That is, as the ClO_x diminishes throughout the study period, the partitioning between ClO and Cl_2O_2 increasingly favors ClO and the apparent decrease in ClO is reduced. Had ClO_x been used in place of ClO in the foregoing analysis, the lack of balance between the decrease in reactive chlorine and the increase in $ClONO_2$ would have been amplified. Another factor which could impact the observed rate of ClO decline is the changing solar zenith angle and local solar time of the measurements. The dimer is cycled back into ClO through the processes of thermal decomposition and photolysis, which is curtailed under low-sunlight conditions. The solar zenith angle at 75°S decreases from ~88° to ~78° in the period after 3 September (cf. Figure 1*b*), leading to increased ClO relative to ClO_x. To address this issue, model results from run D are sampled at local noon (when ClO is expected to be a maximum) at every grid point and compared to those from sampling at the same local time as the measurements (not shown; see *Chipperfield et al.* [1995]). In early September, there is a slight (~0.1 ppbv) difference at both levels in vortex-averaged model ClO between the two sampling strategies which decreases throughout the interval as the local solar time of the MLS measurements in the vortex region shifts from mid-afternoon to late morning. In general, the change in the solar zenith angle has only a small influence on the ClO concentrations (at the solar zenith angles in this study period), and we conclude that it can be safely ignored in analyzing the observations.

Behavior of HCl

As the model results of *Chipperfield et al.* [1995] suggest, $ClONO_2$ may not be the dominant chlorine reservoir during the initial stages of recovery. *Santee et al.* [1995] report that in mid-August 1992, gas-phase HNO_3 values measured by MLS were extremely low ($\leq$ 2 ppbv) throughout a low-temperature ($\leq$ 195 K) region encompassing most of the Antarctic vortex. The deficit in gas-phase HNO_3 persisted into November, well after lower stratospheric temperatures had risen above the PSC evaporation threshold, implying that denitrification had occurred in the polar vortex. Removal of gas-phase HNO_3 prevents NO_2 release from HNO_3 photolysis, and consequently inhibits formation of $ClONO_2$. Detailed modeling simulations [*Prather and Jaffe*, 1990] of perturbed air parcels spun out from the vortex and transported to lower latitudes have shown that when denitrification occurs, $ClONO_2$ is a less significant chlorine reservoir during the first 20 days, and recovery is limited by formation of HCl. Therefore, we consider the possibility that the reactive chlorine is being converted into HCl rather than $ClONO_2$, as seen by *Douglass et al.* [1995].

HALOE observations of HCl become available within the southern polar vortex on about 23 September, a few days after the emission instruments turn away from the south and resume viewing northern high latitudes. HALOE sampling of the southern polar region ceases around 27 October. Individual sunrise or sunset profiles are interpolated to Θ surfaces, and a simple average of all of the profiles falling within the intermediate PV contour shown in Figure 1*a* is calculated. The number of points comprising such a "vortex average" varies with the latitude of the profiles: the maximum number is 15. The daily vortex-averaged mixing ratios at 585 K and 465 K are presented in Figure 10 for the entire period of southern vortex coverage, along with their associated daily average latitudes. Vortex-averaged HCl abundances are seen to increase during this period, particularly at 465 K. Vortex averages of model HCl (which is calculated out through the beginning of October; not shown) agree very well with those of HALOE HCl at

465 K, but underestimate those of HALOE HCl at 585 K by about ().3 ppbv. However, synoptic maps of HCl from the model (Figure 9 of *Chipperfield et al.* [1995]) indicate that the recovery of HCl in the polar region is not homogeneous - at 585 K there is a maximum in model HCl along the vortex edge, with values decreasing toward the vortex center, whereas at 465 1{ the opposite behavior is predicted. Therefore, since the vortex averages in Figures 1 0*a* and 10*b* are based on data from one particular latitude on any given day (see Figure 10*c*), they may not be representative of the vortex HCl as a whole.

Because the HALOE data are strong functions of latitude as well as time, multiple linear regression (with both latitude and time functions included) is used to fit a curve to the daily averages as in *Schoeberl et al.* [1 995]. We initially use the $\partial(HCl)/\partial t$ value obtained from this fit to extrapolate the HCl values back to the timeframe of the MLS and CLAES data. However, at 465 K the change in HCl with time is sufficiently rapid that for most of the interval the extrapolation produces negative mixing ratios. In contrast, at 585 K the change in HCl with timr is so gradual that at the beginning of the interval the extrapolation produces mixing ratios of over 1 ppbv, a value that may be unrealistically high since a substantial fraction of HCl is expected to have been removed by PSC processing at this time. Following the model results presented in Figure 9, which show HCl increasing fairly steadily throughout the interval from near zero at both levels, the HCl is extrapolated back from the first HALOE data point inside the vortex (on 23 September) by assuming it varies linearly from zero at the start of tilt' study period 011 3 September.

In Figure 1 1 we show the vortex- averaged HCl mixing ratios during the HALOE southern vortex sampling period and the linearl - extrapolated HCl values during the late winter study period. Also included in Figure 11 are the adjusted mixing ratios of ClO and $ClONO_2$, the sum $ClO+ClONO_2$, and the s11111 $ClO+ClONO_2$ + extrapolated HCl. At both 585 K and 465 K, the sum $ClO+ClONO_2$ exhibits a decreasing trend over the course of the interval. If $ClONO_2$ and HCl are the primary reservoirs for chlorine at

this time, then $ClO + ClONO_2 + HCl$ should be roughly a conserved quantity. At 585 K, inclusion of HCl (extrapolated from zero on 3 September) leads to an apparent increase in the chlorine budget of almost 0.4 ppbv over the interval, with a final value of ~3.0 ppbv. However, the trend in $ClO + ClONO_2 + HCl$ is highly sensitive to the initial value chosen for the HCl extrapolation). Assuming HCl ~ 1 ppbv on 3 September (the result obtained from the $\partial(HCl)/\partial t$ extrapolation) leads to a value of $ClO + ClONO_2 + HCl$ that decreases slightly over the course of the interval, but has a magnitude of about 3.6 ppbv (more than the estimated total chlorine loading at that level). Assuming HCl=0.5 ppbv on 3 September (a value significantly higher than the model prediction of Figure 9) leads to a fairly constant value of 3.1 ppbv for $ClO + ClONO_2 + HCl$. Thus the chlorine budget can be made to balance at 585 K. At 465 K, although the addition of extrapolated HCl does improve the chlorine balance slightly, the contribution from calculated HCl is not sufficient to offset the observed losses. The quantity $ClO + ClONO_2$ + extrapolated HCl declines slightly over the two week study period, although the uncertainties in these quantities are such that a line with zero slope could be fit to these data points. The imbalance in the decrease in reactive chlorine and the increase in the chlorine reservoirs at 465 K cannot be ameliorated simply by adjusting the extrapolation of the HCl data.

Discussion

The lack of balance between the decrease in ClO and the increase in $ClONO_2$ in the Antarctic vortex may not be unexpected. *Santee et al.* [1995] find evidence for severe denitrification in the 1992 Antarctic vortex. Under highly denitrified conditions, the major source of NO_2 is removed and the reformation of $ClONO_2$ is suppressed. However, if $ClONO_2$ is not playing a primary role, then the free chlorine must either be going into another reservoir or it must be resupplied. *Prather and Jaffe* [1990] show that, under conditions of substantial ozone loss, the chemical system is highly nonlinear and the Cl- ClO- $ClONO_2$ partitioning favors Cl, leading to the preferential formation of HCl.

Douglass et al. [1995] have also recently studied the springtime production of chlorine reservoir species. They use UARS data to constrain a chemical box model, and compare both observations and model results within a narrow annulus just inside the southern vortex boundary (the '(collar)) region) for a 3-month period during the 1992 Antarctic winter to those from a similar region and timespan during the 1991-1992 Arctic winter. Results from model runs at 460 K indicate that, in the absence of denitrification, ozone concentrations dictate which chlorine reservoir dominates in spring. When 03 mixing ratios remain above about 0.5 ppmv, $ClONO_2$ production arising from HNO_3 photolysis occurs rapidly. However, following the arguments of *Prather and Jaffe* [1 990], *Douglass et al.* [1995] find that O_3 mixing ratios below 0.5 ppmv lead to net production of HCl.

The conclusions of *Douglass et al.* [1995] pertain strictly to conditions of mild denitrification (as in the Arctic or the Antarctic collar region) and extremely low ozone (as in the Antarctic in October), and consequently they cannot be applied to the early-to- mid September time period studied here. While a significant reduction in ozone is occurring throughout September 1992, on the last day of our study period (1 7 September) O_3 concentrations are still above 0.5 ppmv in most of the area of the vortex [*Waters et al.*, 1993b], and the vortex- averaged O_3 mixing ratio at 465 K [*Manney et al.*, 1993] is still above 1.5 ppmv. However, the formation of HCl may still be the dominant mechanism for chlorine recovery at this time. Results from the SLIMCAT isentropic chemical transport 11)() del[*Chipperfield et al.*, 1995] show that production of $ClONO_2$ is suppressed and ClO is converted into HCl when the reaction OH + ClO - > HCl + 02 is included as an 8% channel. Nevertheless, the data seem to indicate that the observed decay in enhanced ('lO is not entirely offset by a corresponding increase in 11('l at 465 K.

There are several factors which may account for the apparent lack of balance between the decay of reactive chlorine and the production of chlorine reservoirs at 465 K in the Antarctic vortex. As discussed in connection with Figure 3, there are intermittent localized PSC events at the 465 K level through the end of the study period. Due to the

spacing of the UARS orbit tracks, additional short-lived PSCs with limited geographical extent may have gone undetected. The episodic nature of the PSC activity at the end of southern winter may have created a complicated pattern of recurring chlorine activation and deactivat ion. in fact, vortex- averaged 465 K ClO abundances, while following a genera] downward trend, are observed to oscillate by a t enth of a ppbv or so on t imescales of a few days. It may be that the limited horizontal resolution of the data sets, or the fact that we are examining vortex- averaged quantities at a time when processes are occurring on more localized scales, are obscuring the true behavior of the chlorine spec ies.

Alternatively, the answer may lie in incomplete model chemistry or previously unidentified reservoirs of either active or inactive chlorine. *Toon et al.* [199'2] estimate the total amount of inorganic chlorine from the HF burden measured using an airborne Fourier Transform Infrared (F TIR) spectrometer during AASE II. They then deduct from this value their measured HCl, $ClONO_2$, and HOCl burdens, t o calculate the amount of "missing" chlorine. Comparing this quantity to an estimated ClO column amount derived from the maximum mixing ratio observed during AASE II plus an equal amount of the ClO dimer, they find that the amount of "missing" chlorine indicated by the F TIR measurements exceeds that likely to reside in ClO and Cl_2O_2. Although this result is obtained for the Arctic vort ex, a similar deficit of inorganic chlorine over Antarctica in 1987 is noted by *Toon et al.* [1 989]. *Toon et al.* [1 992] conclude that other unmeasured forms of inorganic chlorine may be present in the winter polar vortex, as suggested by *Sander et al.* [1 w].

Finally, the quality of the data themselves may be hampering the effort to close the chlorine budget. Difficulties in initializing the chemical transport model [*Chipperfield et al.*, 1 995] reveal that the UARS data set is not entirely self-consistent. For example, the total inorganic chlorine derived from CLAES N_2O measurements using an empirical relationship [*Webster et* d., 1993] sign ificantly underestimates the sum of MLS ClO and CLAES $ClONO_2$ at 465 1{. The precision of both the MLS and CLAES data sets is a

limiting factor in the analysis of mixing ratio trends, and it affects our ability to make unequivocal statements about the chlorine budget.

To explore this issue fully requires data extending further into the recovery period. In 1992 the viewing geometry precluded MLS and (.; LAES from making Antarctic measurements during the interval from mid-September through the end of October. By the time solltl)-viewing resumed, ClO was no longer enhanced. Unfortunately, this is the only southern winter for which simultaneous CLAES and MLS data exist; the CLAES supply of cryogen was depleted in May 1993, and there are no CL AES measurements after that time. However, we can use UARS data to investigate the behavior of ClO and the chlorine reservoirs in the northern hemisphere.

1992–1993 Northern Hemisphere Winter

Behavior of C1O and C10N0$_2$

MLS observed lower stratospheric ClO enhanced to greater than 1 ppbv as early as 41)ecember 1992 [*Waters et al.*, 1 993*a*; 1 995*a*], when temperatures briefly fell below the threshold for PSC formation. Temperatures fluctuated around the PSC threshold until late December, after which they were almost continuously below the threshold until late February 1993. When MLS resumed north- viewing measurements in mid-February, lower stratospheric ClO abundances greater than 1 ppbv were seen in most of the vortex region [*Waters et* d., 1993*a*]. We will examine this late winter yaw period (12 February 16 March, 1 993) for chlorine balance. As in the southern hemisphere, CLAES measurements of aerosol extinction (not shown) are examined for evidence of continued heterogeneous chlorine activation]]. Except for a few transient and highly localized events during the third week in February, no significant PSC activity is observed during the northern hemisphere late winter yaw period, and ClO declines throughout this interval.

Maps of MLS ClO for three days at the beginning, middle, and end of the north-

ern hemisphere late winter yaw period are shown in Figure 12*a*. Again, only data from the "day" side of the orbit are included in these maps. The northern hemisphere study period is nearly identical to that of the southern hemisphere in terms of season (days since winter solstice); the measurement solar zenith angles are comparable for each set of selected days (cf. Figures 12*b* and 1*b*). The same three contours of *PV* shown in Figure 1*a* are also superimposed on these maps, but in the northern hemisphere the innermost *PV* contour shrinks considerably over time and is not suitable for vortex averaging. The *PV* contours indicate that the vortex is highly distorted and displaced from the pole throughout this period. Although there are patches in which ClO abundances reach Antarctic levels, ClO is not as uniformly enhanced within the vortex as is observed in the southern hemisphere. In addition, ClO appears to diminish more rapidly at both levels in the northern hemisphere than in the southern hemisphere. At 585 K, chlorine is almost completely deactivated by 1 March. These trends are also evident in Figure 13. Maps of CLAES $ClONO_2$ during the late winter interval are shown in Figure 14. $ClONO_2$ abundances in the Arctic vortex are generally smaller than those in the Antarctic collar region, but there is no pronounced deficit in the vortex interior as there is in the Antarctic (cf. Figure 4). $ClONO_2$ mixing ratios and the area in the region poleward of 52°S with $ClONO_2$ concentrations in excess of 1.5 ppbv (Figure 15) show little (or a slightly decreasing) trend at 585 K; however, in contrast to the south, they increase at 465 K.

Effects of Vertical Transport

Diabatic descent is also expected over the northern polar regions [*Schoeberl and Hartmann*, 1991]. Again, we estimate the vertical velocities at 585 K and 465 K from CLAES measurements of N_2O and CH_4. Daily vortex-averaged (for the intermediate *PV* contour shown in Figure 12*a*) mixing ratios for both tracers are plotted in Figure 16. In the north, the vertical velocities estimated from the two tracers are not consistent at 585 K, with CH_4 indicating descent but N_2O indicating ascent. The cause of this

inconsistency may be that the changes in the daily vortex averages cannot be ascribed solely to vertical motions (au underlying assumption in our calculation of the vertical velocities) since two strong stratospheric warmings during the late-winter yaw period [*Manney et* d., 1 994*d*] lead to increased horizontal mixing [*Manney et* d., 1994*b*]. Based on previous studies [e.g, *S. dioeberl et al.*, 1 992], we assume that descent is occurring at this season, and we neglect the N_2O values in intimating the magnitude of the vertical velocity at 585 K. We find the vortex-averaged descent rate to be 0.1 ± 0.2 11111)/s at 585 1{ and 0.1 ± 0.1 mm/s at 465 K when the trends over the entire yaw period are considered. These values are smaller than estimates of the lower stratospheric vertical velocity (0.6- 0.7 mm/s) in February 1993 obtained from simulated air parcel trajectories [*Manney et al.*, 19946]. They are also smaller than the late winter residual vertical velocities diagnosed from AASE data by *Schoeberl et al.* [1992], which range from 0.6 to 1,0 mm/s between 18 and 22 k m at 70°N, and the average diabatic descent rates in the lower stratospheric vortex computed from NM(temperatures over a five-month period from November through March by *Rosenfield et al.* [1 994] (w 1.13-2 km/month, or ~0.5-0.6 mm/s). Contrary to the calculations of *Rosenfield et 01. [1* 994], our results (and those of *Manney et al.* [1994*b*]) indicate that lower stratospheric vertical velocities arc smaller in the northern hemisphere thau in the southern hemisphere (at least for the late winter time periods considered here).

The estimated changes in ClO and $ClONO_2$ due to vertical transport effects are illustrated in Figure 17. The slight dip apparent in the vortex averaged ClO concentrations just after day 1.5 of the study period (27 February) arises from the fact that measurements obtained in the middle of the yaw cycle have high solar zenith angles. We cannot explain the behavior of the last two $ClONO_2$ data points (14, 16 March); large data gaps exist on surrounding days (13, 15 March), which have 1)('[' 11 excluded from the vortex averages, but the data coverage on 14 and 16 March is adequate. In general, the inferred Arctic vertical velocities are too weak to have a substantial impact, and the

corrections to the observed mixing ratios are small. The implied chemical loss in ClO is approximately 0.2 ± 0.1 ppbv at 585 K and 1.2 ± 0.1 ppbv at 465 K, based on linear fits to the data. There is a corresponding increase in $ClONO_2$ of 0.2 ± 0.1 ppbv at 585 K and 1.0 ± 0.1 ppbv at 465 K. In contrast to the southern polar vortex, in the north the calculated chemical changes in ClO and $ClONO_2$ are balanced (within the uncertainties) at both levels. This result is not highly sensitive to the values of the descent rates; the implied chemical changes in ClO and $ClONO_2$ are still in balance at both levels, within the limits of the uncertainties, even when vertical velocities as large as those estimated by *Schoeberl et al.* [1992] are used.

Behavior of HCl

HALOE observations of HCl become available within the northern polar vortex on about 22 March, a few days after MLS and CLAES resume viewing southern high latitudes. HALOE sampling of the northern polar region ceases around 23 April. In the northern hemisphere, sparse data coverage necessitates averaging the HCl within the outermost PV contour shown in Figure 12*a* (rather than the intermediate PV contour) in order to avoid large gaps in the time series of averaged mixing ratios. The daily vortex-averaged mixing ratios at 585 K and 465 K are presented in Figure 18 for the entire period of northern vortex coverage, along with their associated daily average latitudes. Although HCl exhibits an increasing trend in the weeks after yaw, the increase is much more gradual than that observed in the southern polar region (Figure 10). As in the southern hemisphere, $\partial(HCl)/\partial t$ is calculated through multiple linear regression to account for the latitude dependence of the HALOE data, and used to linearly extrapolate HCl back to the timeframe of the MLS and CLAES data. The extrapolation using the $\partial(HCl)/\partial t$ value leads to HCl mixing ratios on 12 February of about 1.4 ppbv at 585 K and 0.3 ppbv at 465 K, in excellent agreement with the observations from both an aircraft [*Webster et al.*, 1993] and a balloon [*Arnold and Spreng*, 1994] flight on 13 February 1992 during

AASE II.

In Figure 19 we show the vortex-averaged (over the outermost PV contour) HCl mixing ratios during the HALOE northern vortex sampling period and the linearly-extrapolated HCl values during the late-winter yaw period. Also included in this figure are the adjusted vortex-averaged (over the intermediate PV contour) mixing ratios of ClO and $ClONO_2$, the sum ClO + $ClONO_2$, and the sum ClO + $ClONO_2$ + extrapolated HCl. At both levels the sum ClO + $ClONO_2$ appears relatively constant (although it undergoes some oscillation at 465 K). With the contribution from estimated HCl, the quantity ClO + $ClONO_2$ + HCl is essentially constant at 3.1 ppbv at 585 K, and varies slightly around ~2.5 ppbv at 465 K.

Discussion

Manney et al. [1994*c*] show that the 1992-1993 Arctic lower stratospheric vortex is anomalously strong, isolated, and persistent, and is characterized by below-average temperatures. It is thus more "Antarctic-like" than is typical. Although the 1992-1993 winter therefore represents fairly extreme Arctic conditions, the observed depiction of gas-phase HNO_3 is nevertheless considerably smaller than that over Antarctica [*Santee et al.*, 1995]. Gas-phase HNO_3 is evidently present in sufficient quantity to supply NO_2 for the rapid formation of $ClONO_2$. In contrast to the southern hemisphere, we find that the observed late winter decrease in ClO is balanced by a corresponding increase in $ClONO_2$ at both 585 K and 465 K. This conclusion is in good agreement with the results from the AASE, AASE II, and EASOE campaigns outlined in the Introduction.

Summary

We have investigated the recovery of the perturbed chlorine chemistry in the lower stratospheric polar regions of both hemispheres. We have correlated MLS measurements of ClO within the polar vortices with simultaneous and co-located CLAES measurements

of $ClONO_2$. Time series of vortex-averaged mixing ratios at both 585 K and 465 K have been analyzed for approximately month--long intervals during late winter: August 17 - September 17, 1992 in the southern hemisphere and February 11 March 16, 1993 in the northern hemisphere. The magnitude of the diabatic descent at each level has been estimated from CLAES measurements of CH_4 and N_2O and used to adjust the observed mixing ratios for the effects of vertical transport.

In the southern hemisphere, continuing polar stratospheric cloud activity, as evidenced by CLAES measurements of aerosol extinction coefficient, prevented ClO from undergoing sustained decline until the latter half of the study period. Even after the enhanced ClO abundances started to recede, there was no significant chemical change seen in $ClONO_2$ at 465 K, and the $ClONO_2$ at 585 K was observed to decrease. Denitrification is expected to have inhibited the formation of $ClONO_2$ by removing gas-phase HNO_3, the source of NO_2. The observational results have also been compared to those from an isentropic chemical transport model [*Chipperfield et al.*, 1995] which was initialized with UARS data. The model reproduced the MLS ClO abundances and downward trend at 585 K, but underestimated MLS ClO by up to 0.4 ppbv at 465 K. The model also reproduced CLAES $ClONO_2$ fairly well at 585 K, but underestimated it by as much as 0.6 ppbv at 465 K. Inclusion of the $OH + ClO \rightarrow HCl + O_2$ reaction as an 8% channel in the model suppressed the rm'every of $ClONO_2$ (for the time period considered here) and promoted the conversion of ClO to HCl at both ,5851< and 465 K. 11 ALOE measurements of HCl in the southern polar vortex, obtained shortly after the h'11,S and CLAES data, were linearly extrapolated back to the timeframe of the study period. At 585 K, the trend in $ClO + ClONO_2 + HCl$ was found to be highly sensitive to the value to which the HCl was extrapolated on the first day of the interval, and the chlorine budget could be made to balance by setting HCl=0.5 ppbv on that day (3 September). At 465 K, although the addition of extrapolated HCl did improve the chlorine balance, the contribution from calculated HCl was not sufficient to offset the observed losses, and a slight imbalance was

found between the decrease in reactive chlorine and the change in the chlorine reservoirs. The difficulty in closing the chlorine budget at 465 K in the southern hemisphere may have arisen from complications caused by ongoing activation, incomplete photochemical assumptions, or inadequate data quality.

In the northern hemisphere, ClO was not as uniformly enhanced within the vortex as was observed over Antarctica. In addition, ClO appeared to diminish more rapidly at both levels in the north ern hemisphere. Although the 1 992-1993 Arctic lower stratospheric vortex was more "Antarctic-like" than is typical, sufficient gas- phase HNO_3 remained to supply NO_2 for the rapid formation of $ClONO_2$. In contrast to the southern hemisphere, the decrease in ClO at the end of winter was balanced at both 585 K and 465 K by a corresponding increase in $ClONO_2$. We found that $ClONO_2$ was the primary reservoir during recovery in the northern hemisphere, in good agreement with the results from previous Arctic studies.

Acknowledgments. The authors would like to thank our UARS colleagues for their support and their contributions to its success. We are grateful to National Meteorological Center (N MC) Climate Analysis Center personnel, especially M. E. Gelman and A. ,1. Miller, for making NMC data available to the UARS project. We would also like to thank T. Lungu for providing (lO data from the preliminary retrieval algorithms, R.. 1'. Thurstans and B. 1'. Ridenoure for graphics assistance, and 'J'. Luu for data management. Helpful discussions with P. S. Connell, D. E. Kinnison, and G. C. Toon were greatly appreciated. M. L. Santee gratefully acknowledges support from the Resident Research Associateship prog ram of the National Research Council. The work at the Jet Propulsion Laboratory, California Institute of Technology was sponsored by the National Aeronautics and Space Administration and the work at ('ambridge (University forms part of the UK Universities' Global Atmospheric Modelling Programme.

References

Adrian, G. 1'., M. Baumann, 1'. Blumenstock, H. Fischer, A. Friedle, 1,. Gerhardt, G. Maucher, H. Oelhaf, W. Scheuerpflug, P. Thomas, O. Trieschmann and A. Wegner, First results of ground-based FTIR measurements of atmospheric trace gases in North Sweden and Greenland during EASOE, *Geophys. Res. Lett.*, *21*, 1343–1346, 1994.

Anderson, J. G., W, H. Brune and M. 11. Proffitt, Ozone destruction by chlorine radicals within the Antarctic vortex: The spatial and temporal evolution of ClO-O_3 antic orrelation based on in situ ER-2 data, *J. Geophys. Res.*, *94*, 11,465-11,479, 1989.

Anderson, J. G., D. W. Toohey and W. H. Brune, Free radicals within the Antarctic vortex: The role of CFCs in Antarctic ozone loss, *Science*, *251*, 39-46, 1991.

Andrews, D. G., Sorer comparisons between the middle atmosphere dynamics of the southern and northern hemispheres, *Pure Appl. Geophys.*, *130*, 21:3-2:12, 1989.

Arnold, F. and S. Spreng, Balloon-borne mass spectrometer measurements of HCl and HF in the winter Arctic stratosphere, *Geophys. Res. Lett.*, *21*, 1255-1258, 1994.

Barath, F. T., *et al.*, The Upper Atmosphere Research Satellite Microwave Limb Sounder instrument, *J. Geophys. Res.*, *98*, 10,7.5--10,762, 1993.

Bell, W., N. A. Martin, T. D. Gardiner, N. R. Swann, P. 1'. Woods, 1'. F. Fogal and J. W. Waters, Column measurements of stratospheric trace species over Åre, Sweden, in the winter of 1991-1992, *Geophys. Res. Lett.*, *21*, 1347-1350, 1994.

Brune, W. II., J. G. Anderson, and 1<. R. Chan, In Situ Observations of ClO in the Antarctic: ER-2 aircraft results from .540S to 72°S latitude, *J. Geophys. Res.*, *94*, 16,649-16,663, 1989.

Brune, W. 11., J. G. Anderson, D. W. Toohey, D. W. Fahey, S. R. Kawa, R. .. Jones, 1). s. McKenna, and L. R. Poole, The potential for ozone depletion in the Arctic polar stratosphere, *Science*, *252*, 1260 1266, 1991.

Chandra, S., C. H. Jackman, A. R. Douglass, E. L. Fleming, and D. B. Considine, Chlorine catalyzed destruction of ozone: implications for ozone variability in the upper stratosphere, *Geophys. Res. Lett.*, *20*, 351-354, 1993.

Chipperfield, M. P., M. L. Santee, I. Froidevaux, and J. W. Waters, Isentropic 3D chemical transport model and comparison with UARS data in southern polar vortex September 1992, Submitted to *J. Geophys. Res.*, 1995

Coffey, M. T., W. G. Mankin and A. Goldman, Airborne measurements of stratospheric constituents over Antarctica in the austral spring, 1987, 2. Halogen and nitrogen trace species, *J. Geophys. Res.*, *94*, 16,597–16,613, 1989.

Collins, J. E., G. W. Sachse, B. E. Anderson, A. J. Weinheimer, J. G. Walega and B. A. Ridley, AASE II in-situ tracer correlations of methane, nitrous oxide, and ozone as observed aboard the DC-8, *Geophys. Res. Lett.*, *20*, 2543–2546, 1993.

de Zafra, R. L., M. Jaramillo, A. Parrish, P. Solomon, B. Connor, and J. Barrett, High concentrations of chlorine monoxide at low altitudes in the Antarctic spring stratosphere: Diurnal variation, *Nature*, *328*, 408–411, 1987.

Douglass, A. R., M. R. Schoeberl, R. S. Stolarski, J. W. Waters, J. M. Russell III and A. E. Roche, Interhemispheric differences in springtime deactivation of vortex ClO, *Geophys. Res. Lett.*, in press, 1995.

Fahey, D. W., D. M. Murphy, K. K. Kelly, M. K. W. Ko, M. H. Proffitt, C. S. Eubank, G. V. Ferry, M. Loewenstein, and K. R. Chan, Measurements of nitric oxide and total reactive nitrogen in the Antarctic stratosphere: Observations and chemical implications, *J. Geophys. Res.*, *94*, 16,665–16,681, 1989.

Farmer, C. B., G. C. Toon, P. W. Schaper, J.-F. Blavier, and L. L. Lowes, Stratospheric trace gases in the spring 1986 Antarctic atmosphere, *Nature*, *329*, 126–130, 1987

Jones, R. L., J. Austin, D. S. McKenna, J. G. Anderson, D. W. Fahey, C. B. Farmer, L. E. Heidt, K. K. Kelly, D. M. Murphy, M. H. Proffitt, A. F. Tuck, and J. F. Vedder, Lagrangian photochemical modeling studies of the 1987 Antarctic spring vortex, 1. Comparison with AAOE observations, *J. Geophys. Res.*, *94*, 11,529–11,558, 1989

Jones, R. L., D. S. McKenna, L. R. Poole, and S. Solomon, On the influence of polar stratospheric cloud formation on chemical composition during the 1988/89 Arctic winter, *Geophys. Res. Lett.*, *17*, 545–548, 1990.

Kawa, S. R., D. W. Fahey, L. C. Anderson, M. Loewenstein, and K. R. Chan, Measurements

of total reactive nitrogen during the Airborne Arctic. Stratospheric Experiment, *Geophys. Res. Lett.*, *17*, 4X5-488, 1990.

Kawa, S. R., D. W. Fahey, L. E. Heidt, W. 11. Pollock, S. Solomon, D. E. Anderson, M. Loewenstein, M. H. Proffitt, J. J. Margitan, K. R. Chan, Photochemical partitioning of the reactive nitrogen and chlorine reservoirs in the high-latitude stratosphere, *J. Geophys. Res.*, *97*, 7905-7923, 1992.

Kumer, J. B., J. L. Mergenthaler, and A. E. Roche, CLAES CH_4, N_2O, and CCL_2F_2 (F12) global data, *Geophys. Res. Lett.*, 20, 1239-1242, 199:i.

Liu, X., R. D. Blatherwick, F. J. Murcray, J. G. Keys, and S. Solomon, Measurements and model calculations of HCl column amounts and related parameters over McMurdo during the austral spring in 1989, *J. Geophys. Res.*, *97*, 20,795-20,804, 1992.

Loewenstein, M., J. R. Podolske, K. R. Chan and S. E. Strahan, Nitrous oxide as a dynamical tracer in the 1987 Airborne Antarctic Ozone Experiment, *J. Geophys. Res.*, *94*, 11,51S9-11,59s, 1989.

Loewenstein, M., J. R. Podolske, K. R. Chan and S. E. Strahan, N_2O as a dynamical tracer in the Arctic vortex, *Geophys. Res. Lett.*, *17*, 477-480. 1990.

Lutman, E. R., R. Toumi, R. L. Jones, D. J. Lary, J. A. Pyle, Box model studies of ClO_x deactivation and ozone loss during the 1991/92 northern hemisphere winter, *Geophys. Res. Lett.*, *21*, 1415-141s, 1994.

McCormick, M. 1'., C. R. Trepte and M. C. Pitts, Persistence of polar stratospheric clouds in the southern polar region, *J. Geophys. Res.*, *94*, 11,2il-11,251, 1989.

McElroy, M. B. and R. J. Salawitch, Changing composition of the global stratosphere, *Science*, *243*, 763-770, 1989.

McKenna, D. S., R. 1,. Jones, J,. R. Poole, S. Solomon, D. W. Fahey, K. K. Kelly, M. 11. Proffitt, W. 11. Brune, M. Loewenstein, and K. R. Chan, Calculations of ozone destruction during the 1988/89 Arctic winter, *Geophys. Res. Lett.*, *17*, 553-556, 1990.

Mankin, W. G., M. T. Coffey, A. Goldman, M. R. Schoeberl, L. R. Lait, and P. A. Newman, Airborne measurements of stratospheric constituents over the Arctic in the winter of 1989, *Geophys. Res. Lett.*, *17*, 473–476, 1990.

Manney, G. 1,. and R. W. Zurek, Interhemispheric comparison of the development of the stratospheric polar vortex during fall: A 3-dimensional perspective for 199--1992, *Geophys. Res. Lett.*, *20,* 1275-1278, 1993.

Manney, G. L., I,. Froidevaux, J. W. Waters, L. S. Elson, E. F. Fishbein, R. W. Zurek, R. S. Harwood, and W. A. Lahoz, The Evolution of Ozone Observed by UARS MLS in the 1992 late winter southern polar vortex, *Geophys. Res. Lett.*, *20*, 1279-1282, 1993.

Manney, G. 1.,., I,. Froidevaux, J. W. Waters, R. W. Zurek, W. G. Read, L. S. Elson, J. B. Kumer, J. L. Mergenthaler, A. E. Roche, A. O'Neill, R. S. Harwood, 1. MacKenzie and R. Swinbank, Chemical depletion of ozone in the Arctic lower stratosphere during winter 1992-93, *Nature*, *370*, 429-434, 1994*a*.

Manney, G. L., R. W. Zurek, A. O'Neill, and R. Swinbank, On the motion of air through the stratospheric polar vortex, *J. Atmos. Sci.*, 51, 2973-2994, 1994*b*.

Manney, (;. I,., R. W. Zurek, M. E. Gelman, A. J. Miller and R. Nagatani, The anomalous Arctic lower stratospheric polar vortex of 1992-1993, *Geophys. Res. Lett.*, *21*, 2405-2408, 1994(*'*.

Manney, G. 1,., R. W. Zurek, A. O'Neill, R. Swinbank, J. B. Kumer, J. L. Mergenthaler, and A. E. Roche, Stratospheric Warmings during February and March 1993, *Geophys. Res. Lett.*, *21*, 813-816, 1994*d*.

Massie, S. T., J. C. Gille, P. L. Bailey, L. V. Lyjak, C. A. Craig, C. P. Cavanaugh, J. L. Mergenthaler, A. E. Roche, J. B. Kumer, A. Lambert, R. D. Grainger, C. D. Rodgers, F. W. Taylor, J. M. Russell 1[1, J. H. Park, T. Deshler, M. E. Hervig, E. F. Fishbein, J. W. Waters, and W. A. Lahoz, Multi-wavelength (CLAES observations of stratospheric aerosol, Submitted to *J. Geophys. Res.*, 1995.

Mergenthaler, J. L., J. B. Kumer, and A. E. Roche, CLAES south-looking aerosol observations for 1992, *Geophys. Res. Lett.*, *20*, 12951298, 1993.

Mergenthaler, J. 1,., .1. 13. Kumer, A. E. Roche, R. W. Nightingale, J. F. Potter, J. C. Gille, S. T. Massie, 1', L. Bailey, D. Edwards, 1'. S. Connell, D. E. Kinnison, M. R. Gunson, M. C. Abrams, G. C. Toon, B. Sen, ,1.-11'. Blavier, D. G. Murcray, F..1. Murcray, and A. Goldman, Validation of CLAES $ClONO_2$ measurements, Submitted to J. *Geophys. Res.*, 1995.

Minschwaner, K., R. .1. Salawitch, and M. B. McElroy, Absorption of solar radiation by O_2: Implications for O_3 and lifetimes of N_2O, $CFCl_3$, and CF_2Cl_2, *J. Geophys. Res.*, *98*, 10,5zl:\-10,561, 1993.

Molina, I,. '1'. and M. J. Molina, l'reduction of Cl_2O_2 from the self-reaction of the ClO radical, *J. Phys. Chem.*, *91*, 433-436, 1987.

Müller, R., Th. Peter, 1'. J. Crutzen, H. Oelhaf, G. J'. Adrian, Th. v. Clarmann, A. Wegner, U. Schmidt and D. Lary, Chlorine chemistry and the potential for ozone depletion in the Arctic stratosphere in the winter of 1991/92, *Geophys. Res. Lett.*, *21*, 1427- 1430, 1994.

Natarajan, M. and 1.. B. Callis, Stratospheric photochemical studies with Atmospheric Trace Molecule Spectroscopy (ATM(N) measurements, *J. Geophys. Res.*, *96*, *9:161-9370,* 1991.

Oelhaf, 11., T. v. (larmann, H. Fischer, F. Friedl- Vallon, C. Fritzsche, A. Linden, C. Piesch, M. Seefeldner and W. Völker, Stratospheric ($ClONO_2$ and HNO_3 profiles inside the Arctic vortex from M 1 I'AS- B limb emission spectra obtained during EASOE, *Geophys. Res. Lett.*, *21*, 1263- 1266, 1994.

Poole, L. R. and M. C. Pitts, Polar stratospheric cloud climatology based on Stratospheric Aerosol Measurement 11 observations from 1978 to 1989, *J. Geophys. Res.*, *99*, 13,083-13,089, 1994.

I'rather, M. and A. H. Jaffe, Global impact of the Antarctic ozone hole: (hemical propagation, *J. Geophys. Res.*, *95*, 347:3-3492, 1990.

Roche, A. E., J. B. Kumer, J. L. Mergenthaler, G. A. Ely, W. G. Uplinger, J. F. Potter, T. C. James, and I,. W. Sterritt, The Cryogenic Limb Array Etalon Spectrometer (CLAES) on UARS: Experiment description and performance, *J. Geophys. Res.*, *98*, 10,76:3-10,775, 1993*a*.

Roche, A. E., J. B. Kumer, and J. L. Mergenthaler, CLAES observations of $ClONO_2$ and HNO_3 in the Antarctic stratosphere, between June 15 and September 17, 1992, *Geophys. Res. Lett.*, *20*, *122:3-1226,* 199315.

Roche, A. E., J. B. Kumer, J. L. Mergenthaler, R. W. Nightingale, W. G. Uplinger, G. A. Ely, J. F. I'otter, D. J. Wuebbles, 1'. S. Connell, and D. E. Kinnison, Observations of lower-stratospheric $ClONO_2$, HNO_3, and aerosol by the UARS CLAES experiment between January

1992 and April 1993, J. *Atmos. Sci.*, *51*, 2877-2902, 1994.

Roche, A. E., J. B. Kumer, R. W. Nightingale, J. L. Mergenthaler, P. L. Bailey, S. T. Massie, J. C. Gille, M. R. Gunson, M. C. Abrams, G. C. Toon, C. R. Webster, W. A. Traub, K. W. Jucks, D. G. Johnson, R. de Zafra, D. G. Murcray, F. J. Murcray, and A. Goldman, Validation of CH_4 and N_2O measurements by the CLAES instrument on UARS, Submitted to *J. Geophys. Res.*, 1995.

Rosenfield, J. E., P. A. Newman, and M. R. Schoeberl, Computations of diabatic descent in the stratospheric polar vortex, *J. Geophys. Res.*, *99*, 16,677-16,689, 1994.

Russell, J. M. III, L. L. Gordley, J. H. Park, S. R. Drayson, W. D. Hesketh, R. J. Cicerone, A. F. Tuck, J. E. Frederick, J. E. Harries and J. J. Crutzen, The Halogen Occultation Experiment, *J. Geophys. Res.*, *98*, 10,777-10,797, 1993.

Russell, J. M. III, L. E. Deaver, M. Luo, J. H. Park, L. L. Gordley, A. F. Tuck, I. G. Nolt, G. C. Toon, M. R. Gunson, W. A. Traub, D. G. Johnson, K. W. Jucks, D. G. Murcray, R. Zander, and C. R. Webster, Validation of hydrogen chloride measurements made by HALOE from the UARS platform, Submitted to *J. Geophys. Res.*, 1995.

Salawitch, R. J., M. B. McElroy, J. M. Yatteau, S. C. Wofsy, M. R. Schoeberl, L. R. Lait, P. A. Newman, K. R. Chan, M. Loewenstein, J. R. Podolske, S. E. Strahan, and M. H. Proffitt, Loss of ozone in the Arctic vortex for the winter of 1989, *Geophys. Res. Lett.*, *17*, .561-564, 1990.

Salawitch, R. J., S. C. Wofsy, E. W. Gottlieb, L. R. Lait, P. A. Newman, M. R. Schoeberl, M. Loewenstein, J. R. Podolske, S. E. Strahan, M. H. Proffitt, C. R. Webster, R. D. May, D. W. Fahey, D. Baumgardner, J. E. Dye, J. C. Wilson, K. K. Kelly, J. W. Elkins, K. R. Chan, and J. G. Anderson, Chemical loss of ozone in the Arctic polar vortex in the winter of 1991-1992, *Science*, *261*, 1146-1149, 1993.

Sander, S. P., R. R. Friedl, and Y. L. Yung, Rate of formation of the $ClO Cl_2O_2$ in the polar stratosphere: Implications for ozone loss, *Science*, *245*, 1095 1098, 1989.

Santee, M. L., W. G. Read, J. W. Waters, L. Froidevaux, G. L. Manney, D. A. Flower, R. F. Jarnot, R. S. Harwood and G. E. Peckham, Interhemispheric differences in polar stratospheric HNO_3, H_2O, ClO, and O_3, *Science*, *267*, 849-852, 1995.

Schoeberl, M. R., M. H. Proffitt, K. K. Kelly, L. R. Lait, P. A. Newman, J. E. Rosenfield, M. Loewenstein, J. R. Podolske, S. E. Strahan, and K. R. Chan, Stratospheric constituent trends from ER-2 profile data, *Geophys. Res. Lett.*, *17*, 469--472, 1990.

Schoeberl, M. R. and D. L. Hartmann, The dynamics of the stratospheric polar vortex and its relation to springtime ozone depletions, *Science*, *251*, 46-52, 1991.

Schoeberl, M. R., L. R. Lait, P. A. Newman, and J. E. Rosenfield, The structure of the polar vortex, *J. Geophys. Res.*, *97*, 7859--78%2, 1992.

Schoeberl, M. R., A. R. Douglass, R. S. Stolarski, P. A. Newman, L. R. Lait, D. Toohey, L. Avallone, J. G. Anderson, W. Brune, D. W. Fahey and K. Kelly, The evolution of ClO and NO along air parer] trajectories, *Geophys. Res. Lett.*, *20*, 2511-2514, 1 993.

Schoeberl, M. R., M. Luo and J. E. Rosenfield, An analysis of the Antarctic HALOE trace gas observations, *J. Geophys. Res.*, in press, 1995.

Solomon, **S.,** The Mystery of the Antarctic ozone "hole'), *Rev. Geophys.*, 26, 131-148, 1988.

Solomon , s., Progress **towards a quantitative** understanding of Antarctic ozone **depletion,** *Nature*, *347*, 347-354, 1990.

Toohey, D. W., L. M. Avallone, L. R. Lait, P. A. Newman, M. R. Schoeberl, D. W. Fahey, E. L. Woodbridge and J. G. Anderson, The seasonal evolution of reactive chlorine in the northern hemisphere stratosphere, *Science*, *261*, 1134-11:16, 1993.

Toon, G. C., C. B. Farmer, L. L. Lowes, P. W. Schaper, J.-F. Blavier, and R. H. Norton, Infrared aircraft measurements of stratospheric composition over Antarctica during September 1987, *J. Geophys. Res.*, *94*, 16,571-16,596, 1989.

Toon, G. C., C. B. Farmer, J. N. Solario, and J. T. Szeto, Airborne observations of the 1992 Arctic winter stratosphere by FTIR solar absorption spectroscopy, *SPIE*, *1715*, 457-467, 1992.

Traub, W. A., K. W. Jucks, D. G. Johnson, and K. V. Chance, Chemical change in the Arctic vortex during AASE 11, *Geophys. Res. Lett.*, *21*, 2595–2598, 1994.

Tuomi, R. and S. Bekki, The importance of the reactions between 011 and ClO for stratospheric ozone, *Geophys. Res. 1X11.*, *20*, 2447--2450, 199:3.

Turco, R. P., O. B. Toon, and P. Hamill, Heterogeneous physicochemistry of the polar ozone

hole, *J. Geophys. Res.* , *94*, 16,493–16,510, 1989.

Waters, J, W., Microwave Limb Sounding, in *Atmospheric Remote Sensing by Microwave Radiometry*, edited by M. A. J anssen, pp. 383–496, Wiley and Sons, 1993.

Waters, J. W., L. Froidevaux, W. G. Read, G. L. Manney, L. S. Elson, D. A. Flower, R. F. Jarnot, and R. S. Harwood, Stratospheric ClO and ozone from the Microwave Limb Sounder on the Upper Atmosphere Research Satellite, *Nature*, *362*, 597--602, 1993*a*.

Waters, J. W., L. Froidevaux, G. L. Manney, W. G. Read, and L. S. Elson, MLS observations of lower stratospheric ClO and O_3 in the 1992 southern hemisphere winter, *Geophys. Res. Lett.*, *20*, 1219-1222, 1993*b*.

Waters, J. W., G. J,. Manney, W. G. Read, L. Froidevaux, D. A. Flower, R. F. Jarnot, UARS MLS observations of lower stratospheric ClO in the 1992- 93 and 199:1-94 Arctic winter vortices, *Geophys. Res. Let 1.*, *xx*, yyyy - zzzz, 1995*a*.

Waters, J. W., W. G. Read, L. Froidevaux, T. A. Lungu, V. S. Perun, R. A. Stachnik, R. F. Jarnot, R. E. Cofield, E. F. Fishbein, 1.). A. Flower, J. R. Burke, J. C. Hardy, L. L. Nakamura, B. P. Ridenoure, Z. Shippony, R. P. Thurstans, L. M. Avallone, D. W. Toohey, R. L. de Zafra, 1). T. Shindell, Validation of UARS M LS ClO Measurements, J. *Geophys. Res.*, *xxx*, yyyy - zzzz, 1995*b*.

Webster, C. R., R. D. May, D. W. Toohey, L. M. Avallone, J. G. Anderson, P. Newman, L. Lait, M. R. Schoeberl, J. W. Elkins and K. R. Chan, Chlorine chemistry on polar stratospheric cloud particles in the Arctic winter, *Science*, *261*, 1130- 1134, 1993.

World Meteorological Organization, Scientific assessment of ozone depletion: 1991, Rep. *25*, Global Ozone Res. and Monit. Proj., Geneva, 1991.

This manuscript was prepared with the AGU LaTeX macros v3.1.

Figure 1a. Maps of MLS ClO for selected days during the 1992 southern hemisphere late winter south-looking period, interpolated onto the 585 K and 465 K potential temperature surfaces using NMC temperatures. The maps are polar orthographic projections extending to the equator, with the Greenwich meridian at the top and dashed black circles at 30°S and 60°S, and are produced from measurements taken over a 24-hour period. No measurements were obtained in the white area poleward of 80° S. Only data from the "day" side of the orbit are shown. Superimposed in white on each of the maps are three contours of potential vorticity: $-0.70 \times 10^{-4} Km^2 kg^{-1} s^{-1}$, $-1.05 \times 10^{-4} Km^2 kg^{-1} s^{-1}$, and $-1.40 \times 10^{-4} Km^2 kg^{-1} s^{-1}$ at 585 K, and $-0.25 \times 10^{-4} Km^2 kg^{-1} s^{-1}$, $-0.375 \times 10^{-4} Km^2 kg^{-1} s^{-1}$, and $-0.50 \times 10^{-4} Km^2 kg^{-1} s^{-1}$ at 465 K.

Figure 1b. Maps of the solar zenith angle (*sza*) of the MLS measurements ("day" side of the orbit) for the days shown in Figure 1*a*. The 94° *sza* contour represents the approximate edge of daylight for the measurements.

Figure 2. The area in percent of a hemisphere, as a function of potential temperature and time for the 1992 southern hemisphere late winter south-looking period, within which daytime MLS ClO mixing ratios in the region poleward of 52°S exceed 1 ppbv. Tick marks on the vertical axis are not evenly spaced; they represent potential temperature values of 420 K, 465 K, 520 K, 585 K, 655 K, 740 K and 840 K.

Figure 3. The area in percent of a hemisphere as a function of potential temperature and time for the 1992 southern hemisphere late winter south-looking period, within which CLAES aerosol extinction coefficients in the region poleward of 52°S exceed 1.0 $\times 10^{-3}$ km^{-1}. Data gaps (white spaces in plots) occur during the implementation of instrument modes other than normal science operations.

Figure 4. As in Figure 1*a* (with a different color scale), for CLAES $ClONO_2$. Blank spaces in the maps represent areas where there are data gaps or spurious data points.

Figure 5. As in Figure 2 (with a different color scale), for $ClONO_2$ mixing ratios in excess of 1.5 ppbv. Data gaps (white spaces in plots) occur during the implementation of instrument modes other than normal science operations.

Figure 6. Time series, over the latter half of the 1992 southern hemisphere late winter south-looking period (starting on 3 September), of vortex-averaged (using the intermediate *PV* contour shown in Figure 1 a - see text) mixing ratios of CLAES CH_4 (ppmv) and N_2O (ppbv) at 585 K and 465 K. The vortex- averaged values for each day are represented by colored circles (black = CH_4, magenta = N_2O), and the lines are the least-squares fits through the data. The slopes of the lines, in combination with the vertical profiles of CH_4 and N_2O, lead to estimates of the diabatic descent rate of 0.5 + 0.3 mm/s at 585 K and 0.74 0.2 mm/s at 465 K.

Figure 7. Vertical profiles of ClO (a) and $ClONO_2$ (*b*) as a function of potential temperature. These profiles were obtained by averaging individual retrievals both spatially (within the area enclosed by the intermediate *PV* contour of Figure 1*a*) and temporally (over 3-17 September).

Figure 8. Time series, over the latter half of the 1992 southern hemisphere late winter south-looking period (starting on 3 September), of vortex-averaged (using the intermediate *PV* contour shown in Figure 1*a*) mixing ratios of MLS ClO (ppbv) and CLAES $ClONO_2$ (ppbv) at 585 K and 465 K. The vortex-averaged values observed on each day are represented by open triangles, and the mixing ratios adjusted for the effects of diabatic descent are given by solid circles.

Figure 9. Vortex-averaged chlorine species at (*a*) 585 K and (*b*) 465 K from the chemical transport 1I1OCICI. Solid lines denote model species sampled at 1200UT; dashed lines denote model species sampled at the same local time as the MLS and CLAES measurements. During the course of the day, the vortex moves relative to the *PV* contour (fixed at 1200UT) used here to delimit the area over which vortex averages are taken. This occasionally causes model ClO sampled at the MLS local time to exceed model ClO_x sampled at 1200UT. The curves representing model ClO sampled at 1200UT (not shown) and model ClO_x sampled at 1200UT do not cross. Also shown are the MLS ClO and CLAES $ClONO_2$ values. These differ slightly from the vortex averages shown in Figure 8 because they are calculated from the ClO and $ClONO_2$ fields interpolated onto the model T42 Gaussian grid.

Figure 10. Time series, over the HALOE 1992 southern vortex sampling period, of vortex-averaged (within the intermediate *PV* contour) mixing ratios of HALOE HCl (ppbv) at (*a*) 585 K and (*b*) 465 K. The associated daily average latitudes of the profiles are shown in (*c*) (open squares = 465 K, solid circles = 585 K). HALOE data are strong functions of both latitude and time, and multiple linear regression is used to fit curves (solid lines) to the daily averages at both levels.

Figure 11. Vortex-averaged HCl mixing ratios during, the HALOE 1992 southern vortex sampling period (green circles); linearly-extrapolated 11(:1 values (see text) during the latter half Of the late-winter yaw period (dotted green line); adjusted vortex averaged mixing ratios of MLS ClO (red circles) and CLAES $ClONO_2$ (cyan circles); the sum (ClO + $ClONO_2$ (black circles); and the quantity ClO + $ClONO_2$ + extrapolated HCl (magenta pluses).

Figure 12a. As in Figure 10, for the 1992-1993 northern hemisphere late winter north-looking period, with the Greenwich meridian at the bottom, and positive *PV* contour values.

Figure 12b. As in Figure 1*b*, for the days shown in Figure 12*a*.

Figure 13. As in Figure 2 (with a different color scale), for the 1992-1993 northern hemisphere late winter north-looking period.

Figure 14. As in Figure 12*a*, for CLAES $ClONO_2$. Blank spaces in the maps represent areas where three are data gaps or spurious data points.

Figure 15. As in Figure 13, for $ClONO_2$ mixing ratios in excess of 1.5 ppbv. Data gaps (white spaces in plots) occur during the implementation of instrument modes other than normal science operations.

Figure 16. As in Figure 6, for the 1992-1993 northern hemisphere late winter north--looking period. The slopes of the lines lead to estimates of the diabatic vertical velocity of 0.1 $\pm$0.2 mm/s at 585 K and 0.1 $\pm$ 0.1 mm/s at 465 K.

Figure 17. As in Figure 8, for the 1992-1993 northern hemisphere late winter north- looking period.

Figure 18. As in Figure 10, for tile HALOE 1992-199:3 northern vortex sampling period. In this case, averages are computed over the entire vortex region (see text).

Figure 19. As in Figure 11, for the northern hemisphere.

MLS C1O

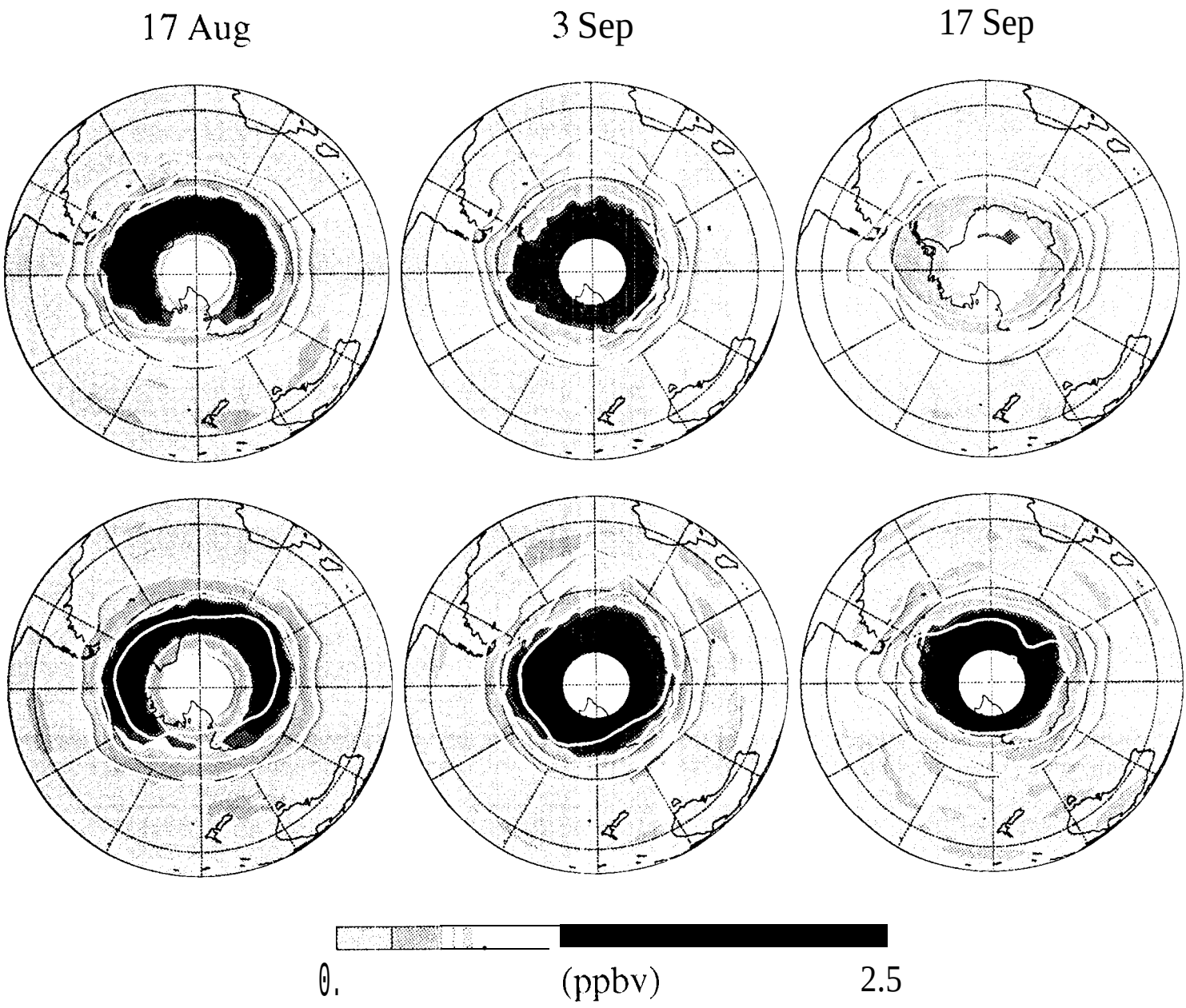

Figure 1.a

Solar Zenith Angle

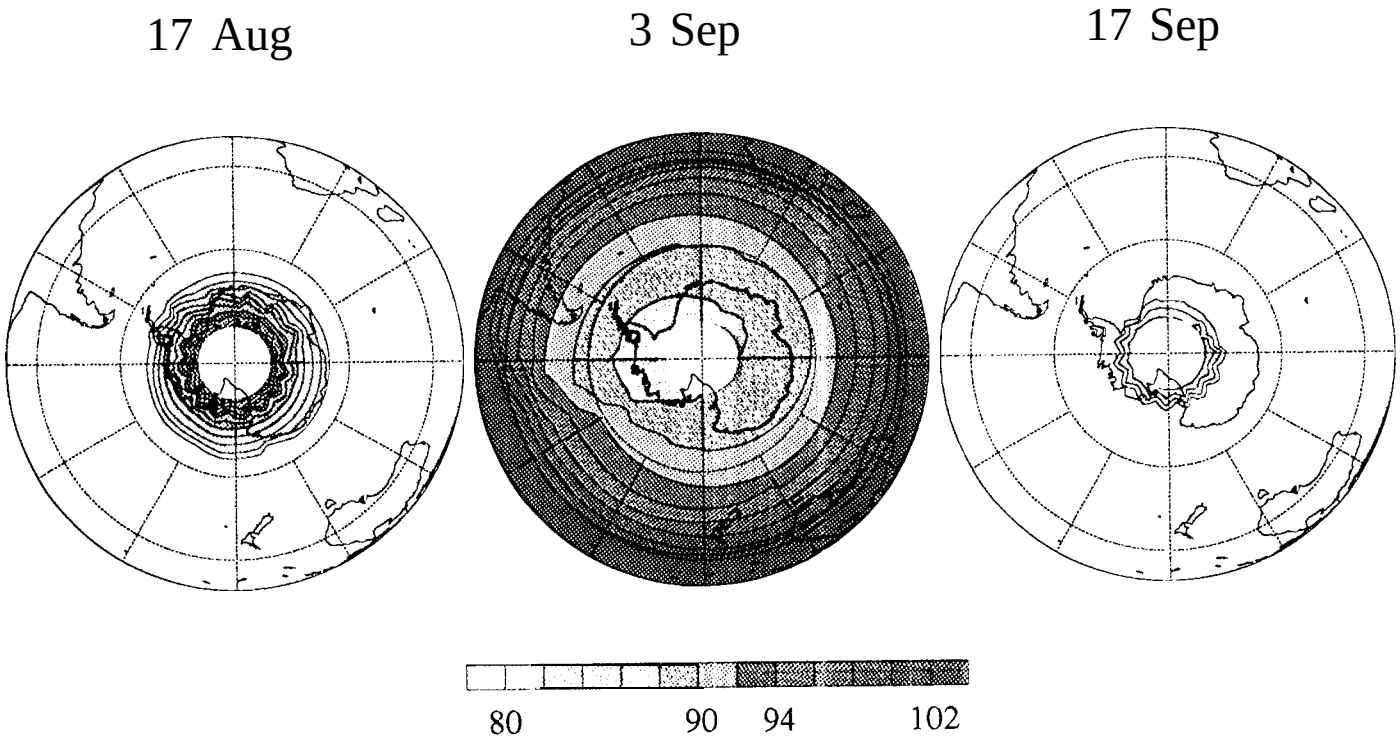

Figure 1b

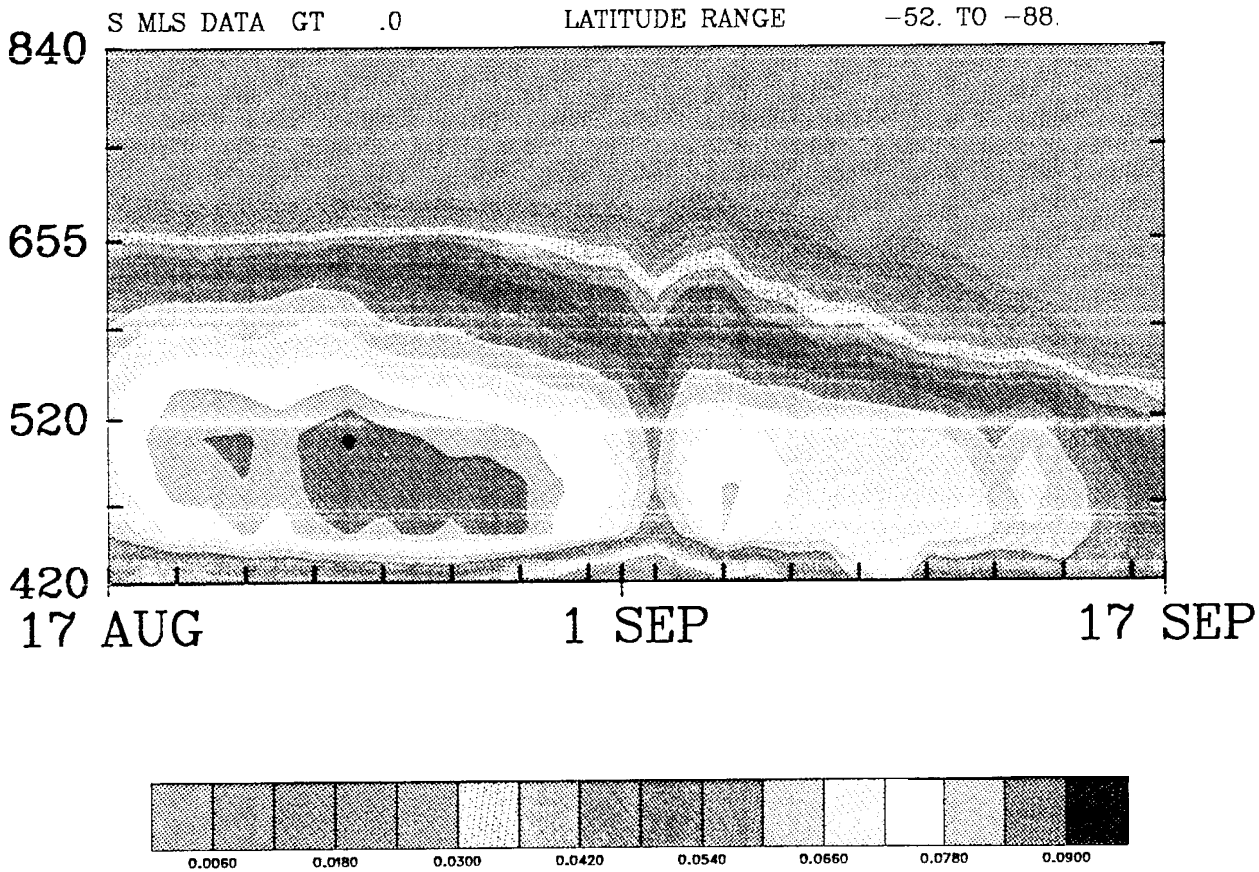
S MLS DATA GT .0
LATITUDE RANGE -52. TO -88.
840
655
520
420
17 AUG
1 SEP
17 SEP
0.0060
0.0180
0.0300
0.0420
0.0540
0.0660
0.0780
0.0900

Figure 2.

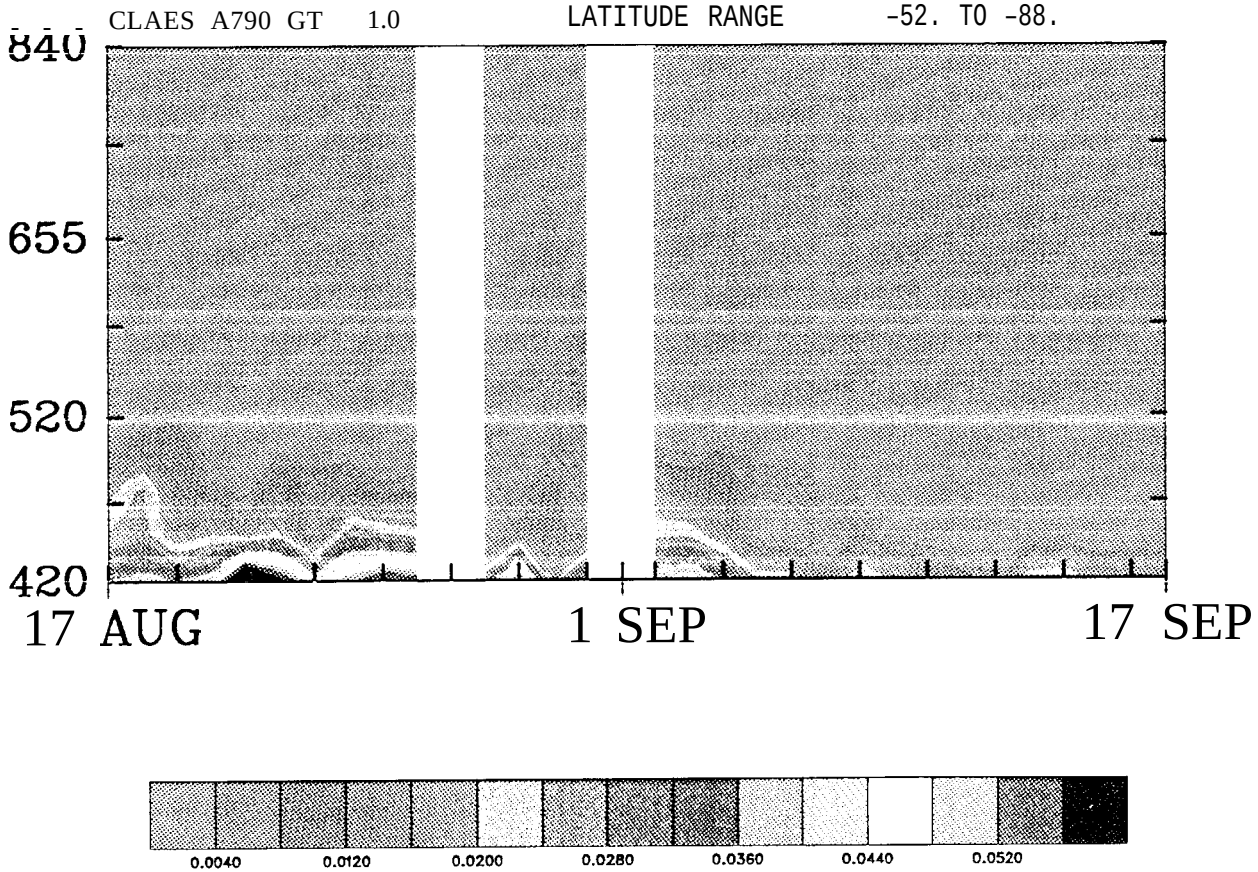
CLAES A790 GT 1.0
LATITUDE RANGE -52. TO -88.
840
655
520
420
17 AUG
1 SEP
17 SEP
0.0040
0.0120
0.0200
0.0280
0.0360
0.0440
0.0520

Figure 3

CLAES $C10N0_2$

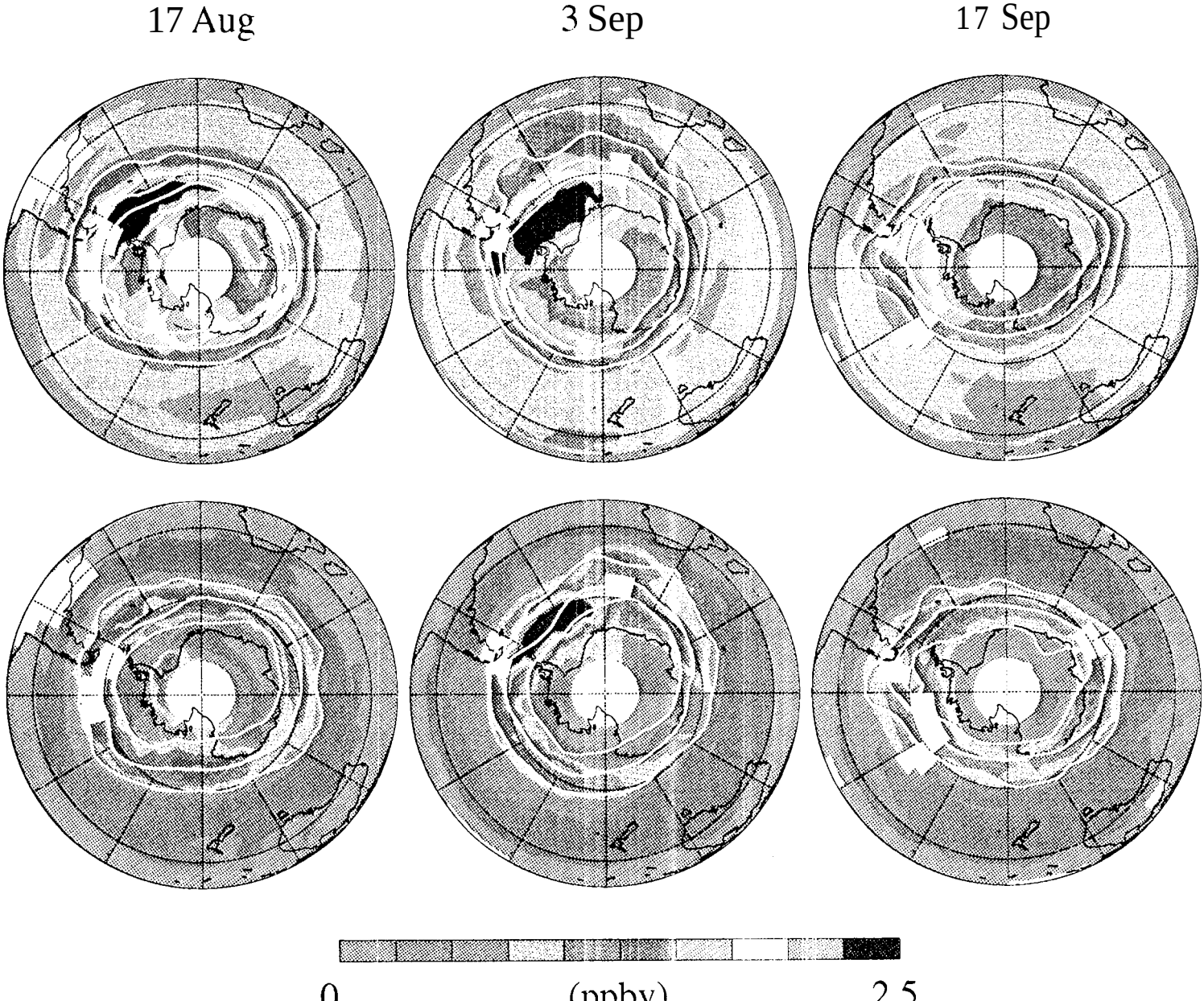

Figure 4

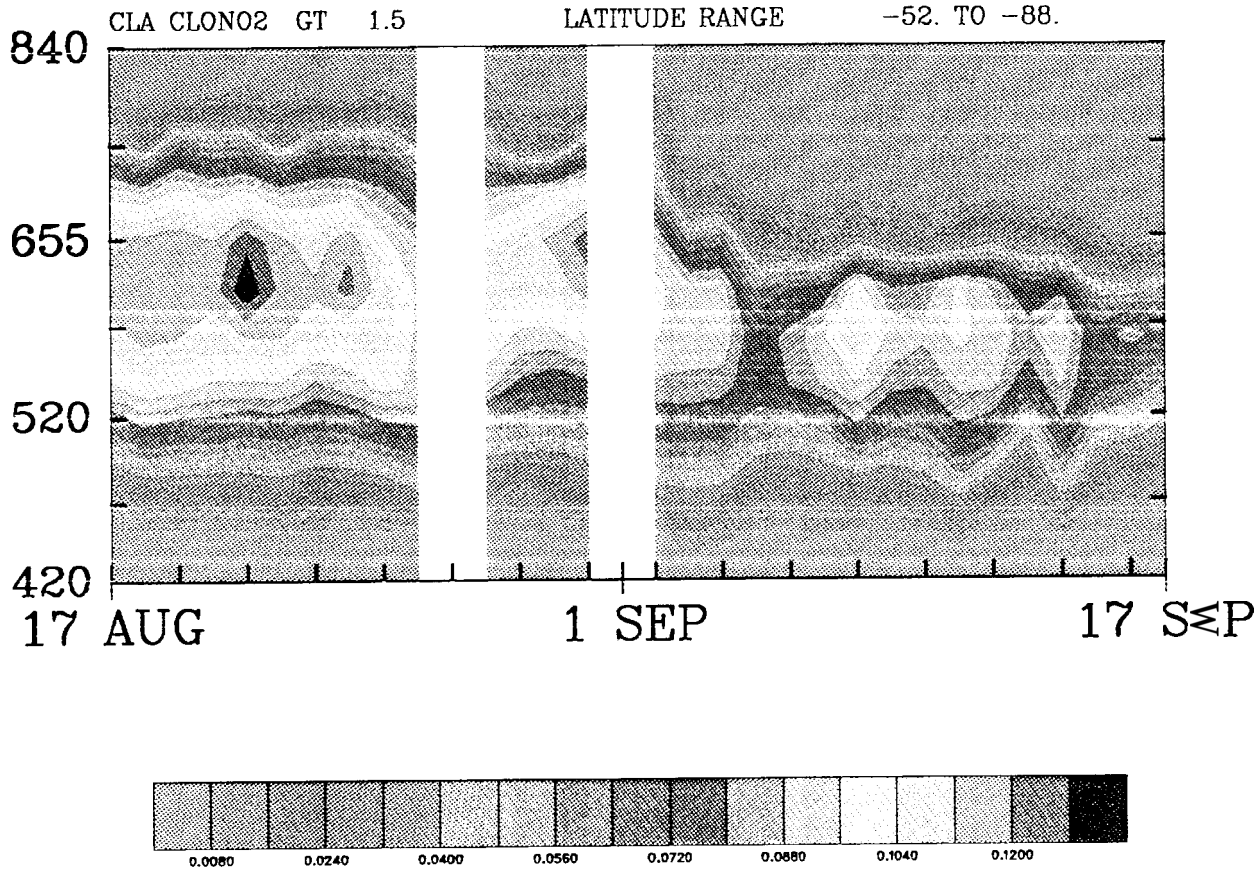
CLA CLONO2 GT 1.5
LATITUDE RANGE -52. TO -88.
840
655
520
420
17 AUG
1 SEP
17 SEP
0.0080
0.0240
0.0400
0.0560
0.0720
0.0880
0.1040
0.1200

Figure 5

585 K
pv=1.050

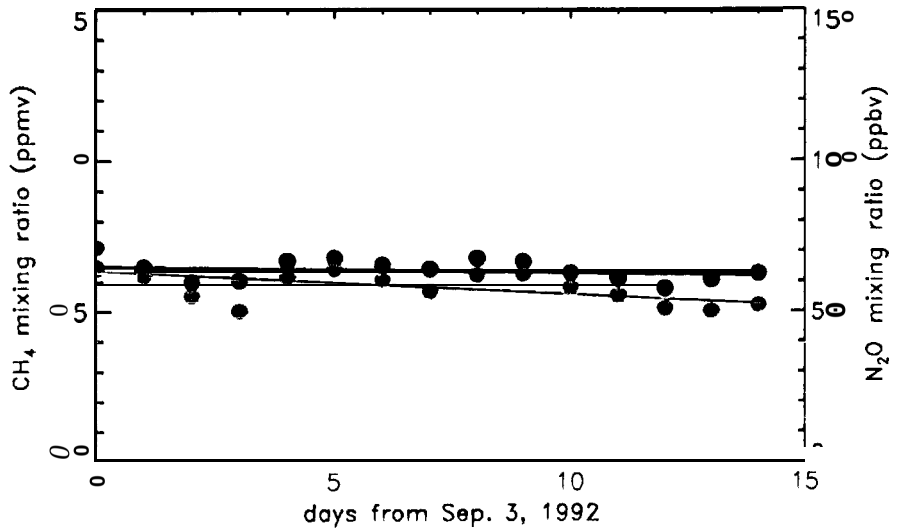

465 K
pv=0.375

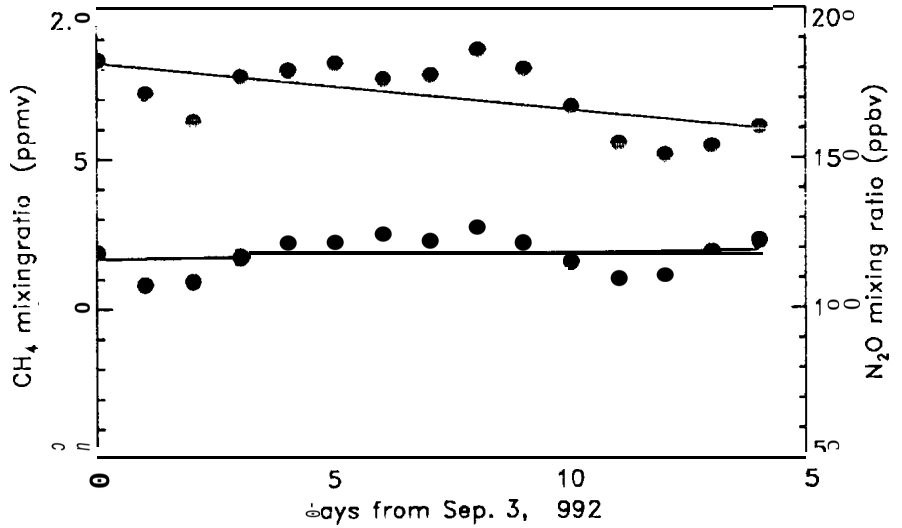

FIGURE 6

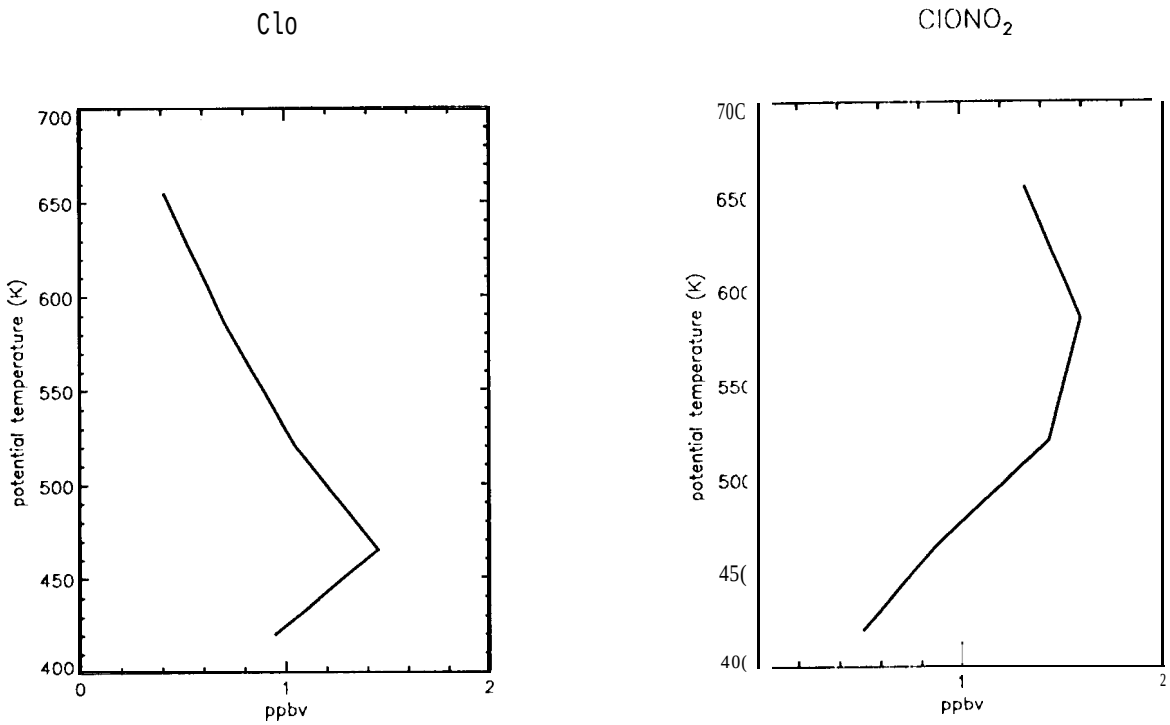
ClO
ClONO2
potential temperature (K)
700
650
600
550
500
450
400
0
1
2
ppbv
70(
65(
60(
55(
50(
45(
40(
1
2
ppbv

FIGURE 7a,b

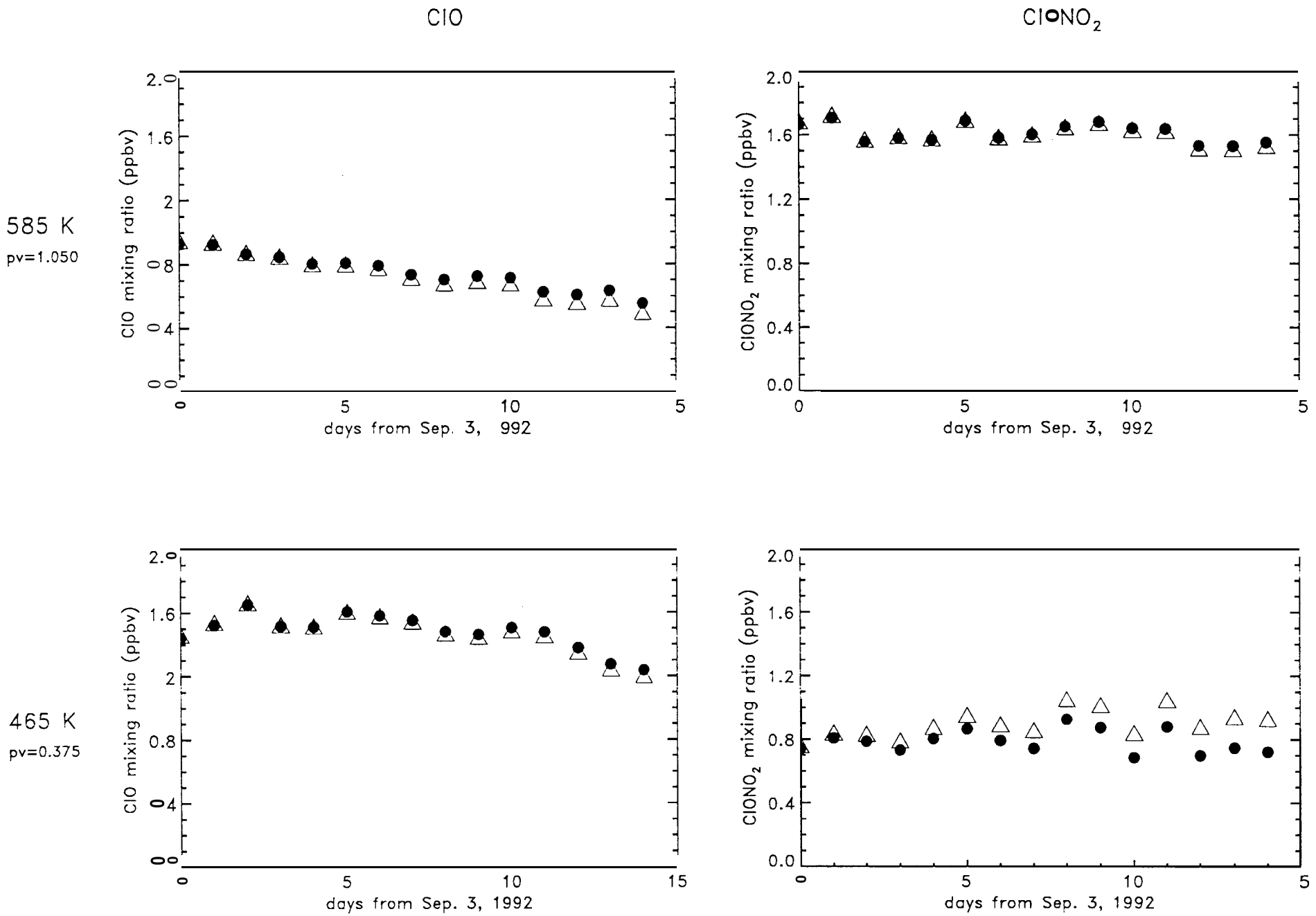
ClO
ClONO2
585 K
pv=1.050
465 K
pv=0.375
ClO mixing ratio (ppbv)
ClONO2 mixing ratio (ppbv)
days from Sep. 3, 992
days from Sep. 3, 1992

FIGURE 8

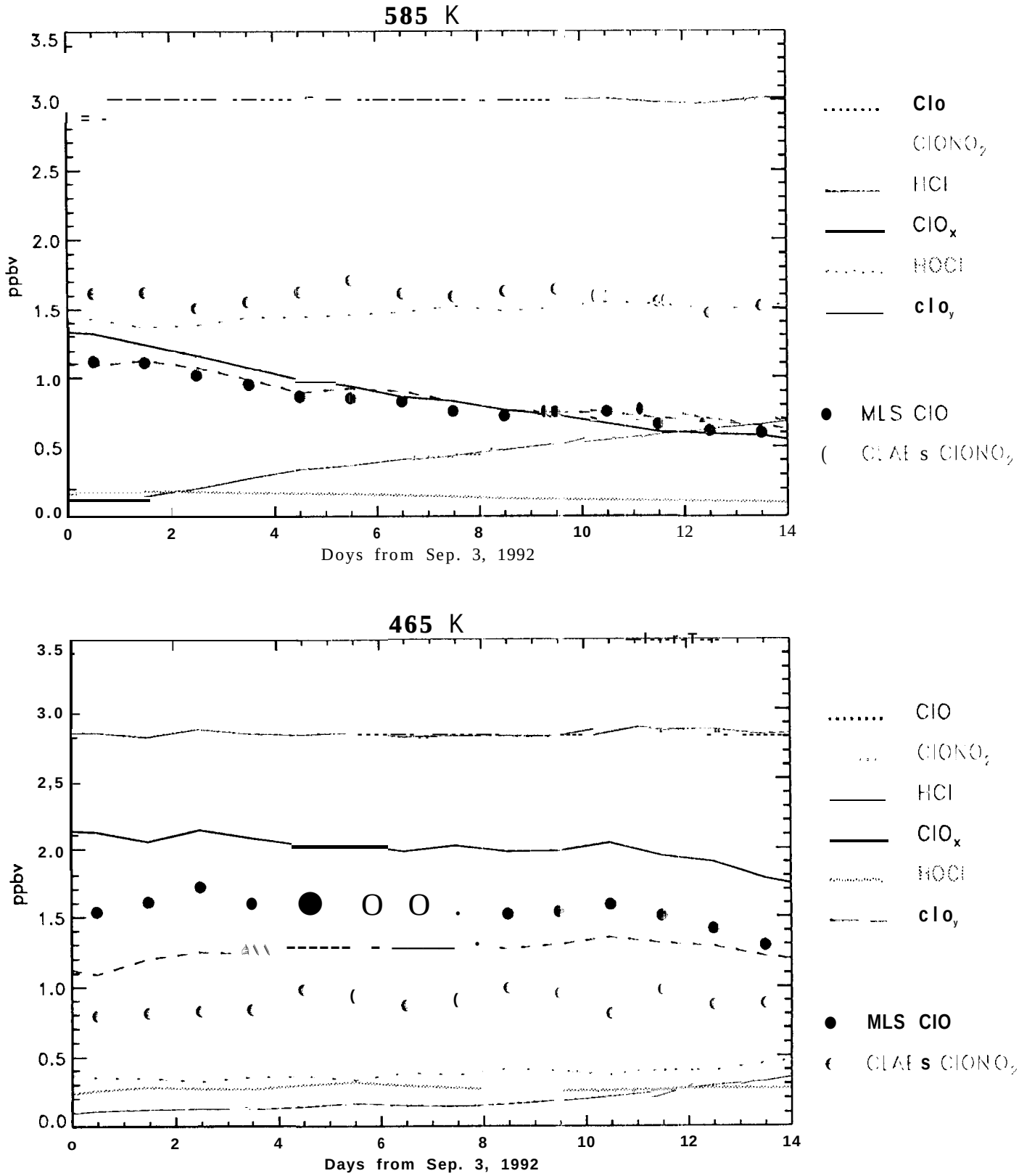
585 K
3.5
3.0
2.5
2.0
1.5
1.0
0.5
0.0
ppbv
0
2
4
6
8
10
12
14
Doys from Sep. 3, 1992
ClO
ClONO2
HCl
ClOx
HOCl
cloy
MLS ClO
CLAES ClONO2
465 K
3.5
3.0
2,5
2.0
1.5
1.0
0.5
0.0
ppbv
o
2
4
6
8
10
12
14
Days from Sep. 3, 1992
ClO
ClONO2
HCl
ClOx
HOCl
cloy
MLS ClO
CLAES ClONO2

Figure 9

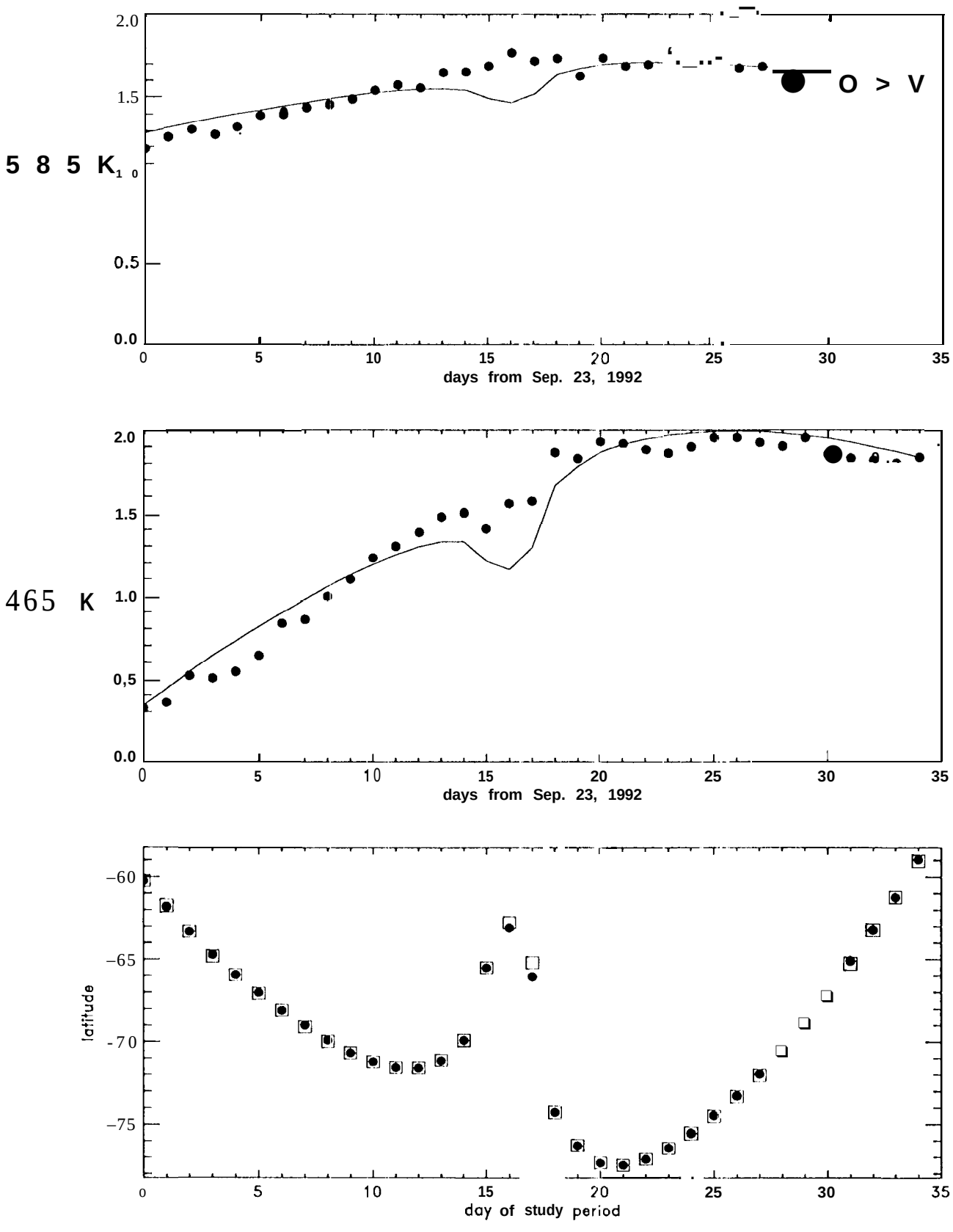
Daily–averaged HCl inside vortex
585 K
O > V
2.0
1.5
0.5
0.0
0
5
10
15
20
25
30
35
days from Sep. 23, 1992
465 K
2.0
1.5
1.0
0,5
0.0
0
5
10
15
20
25
30
35
days from Sep. 23, 1992
latitude
–60
–65
-70
–75
0
5
10
15
20
25
30
35
day of study period

Figure 10

585 K
pv=1.050

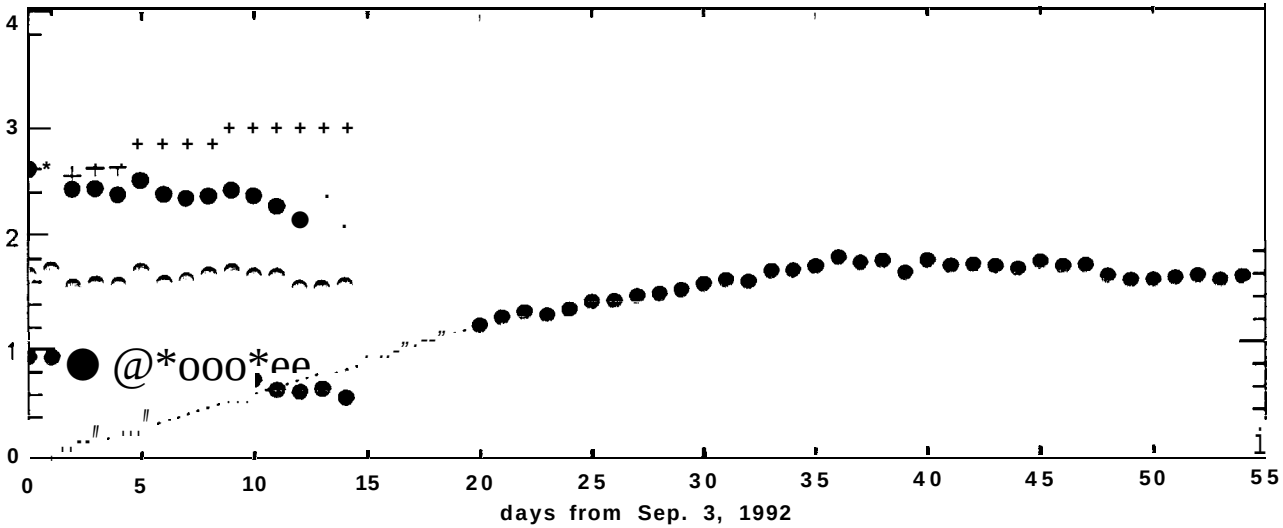

465 K
pv=o.375

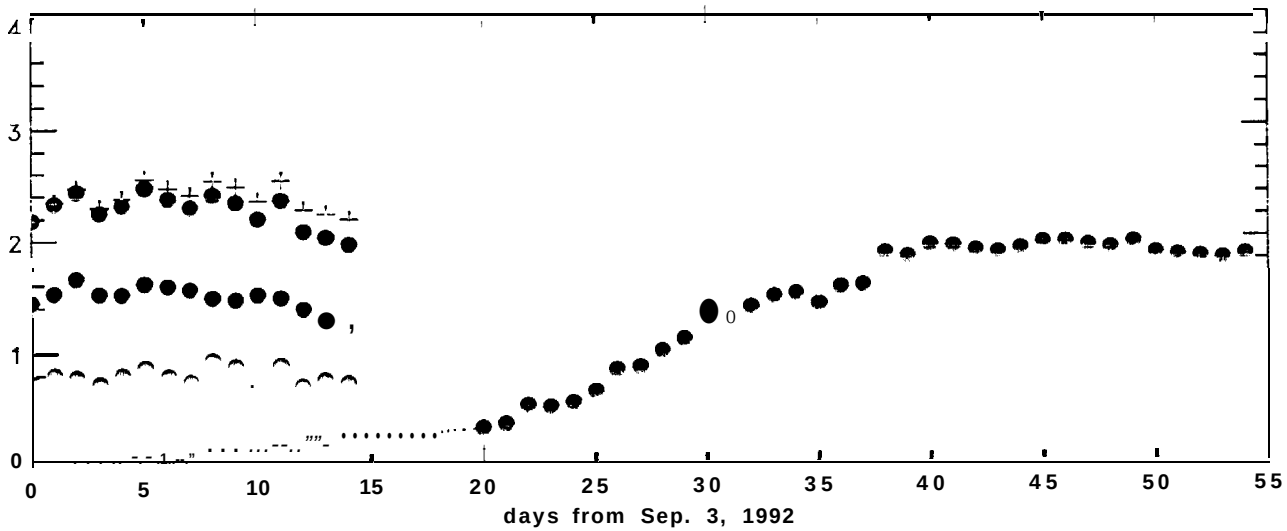

Figure 11

MLS C1O

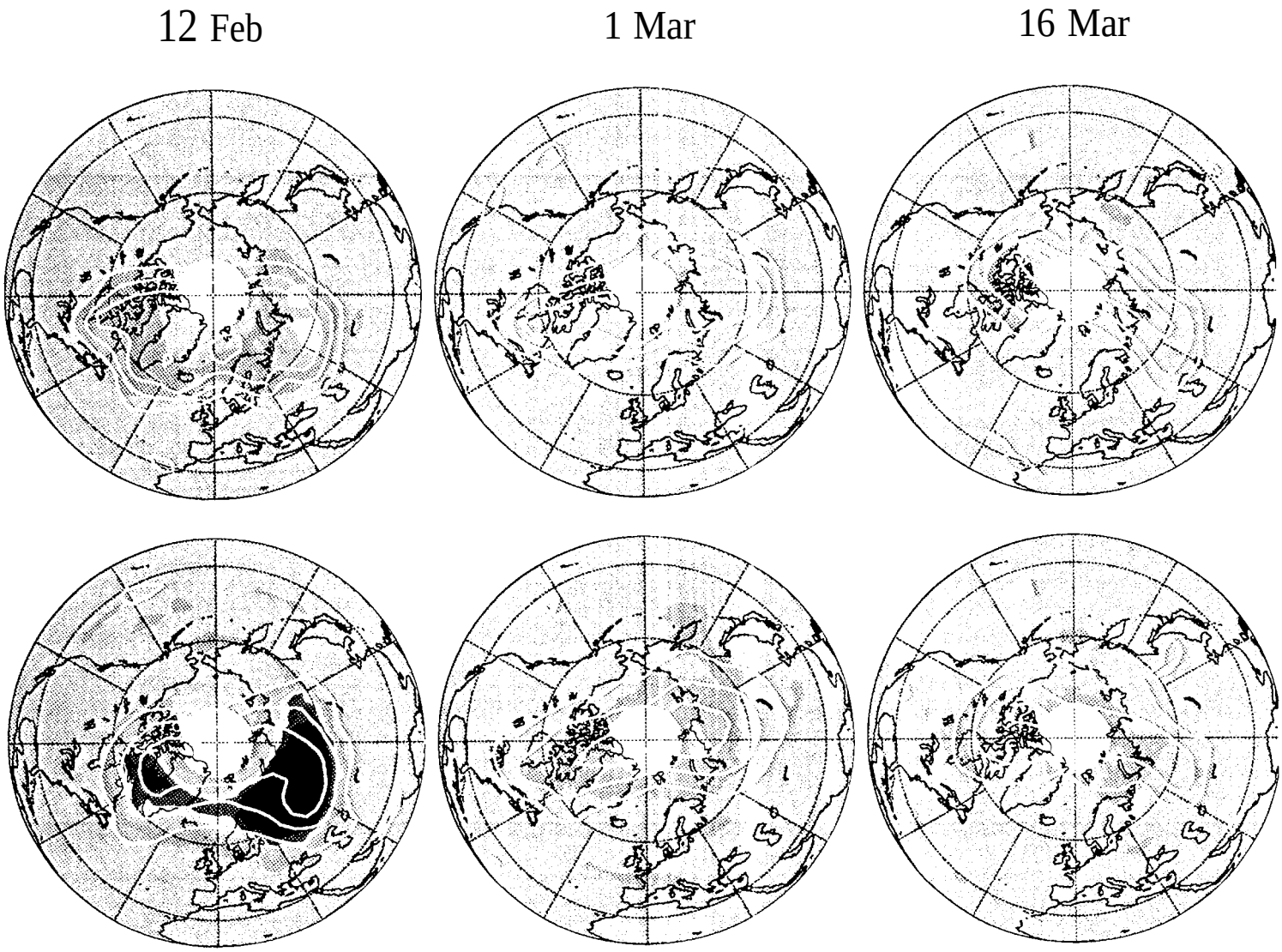

Figure 12a

Solar Zenith Angle

12 Feb

1 Mar

16 Mar

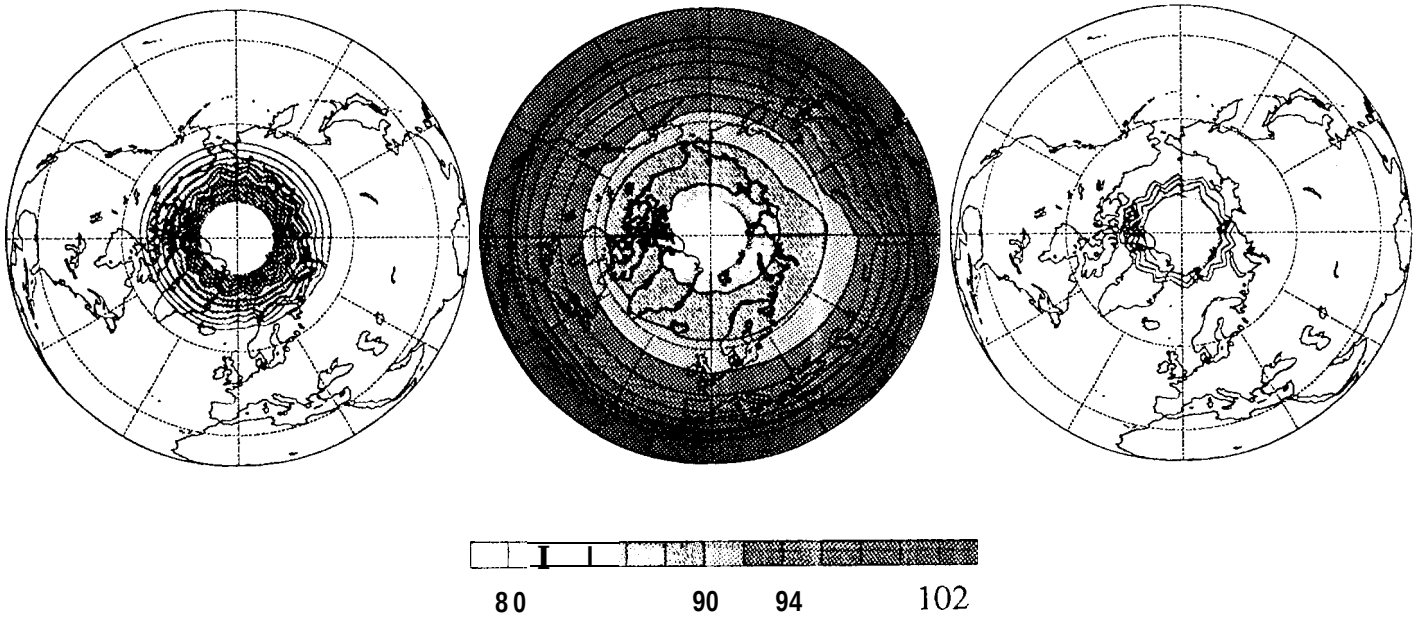

Figure 12b

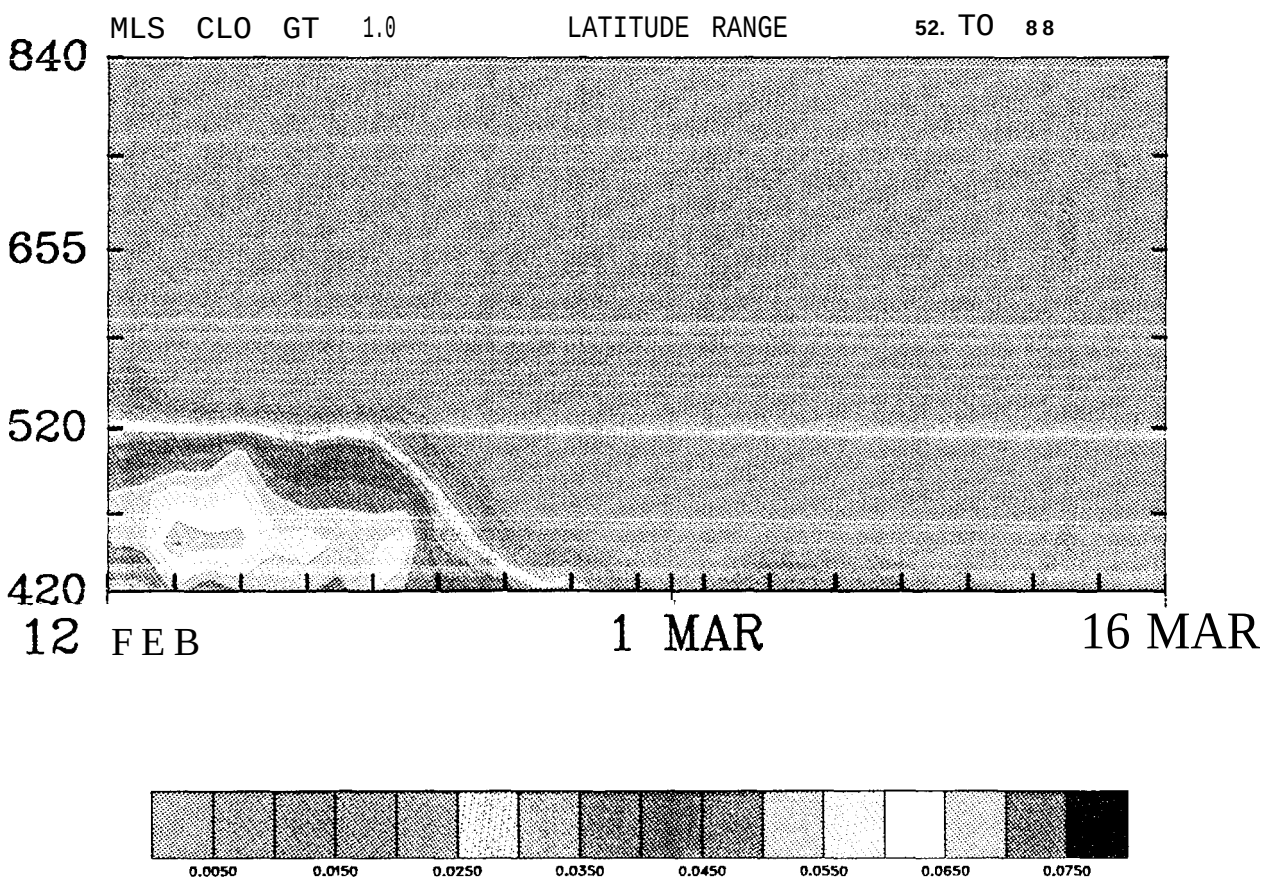
MLS CLO GT 1.0
LATITUDE RANGE 52. TO 88
840
655
520
420
12 FEB
1 MAR
16 MAR
0.0050
0.0150
0.0250
0.0350
0.0450
0.0550
0.0650
0.0750

Figure 13

CLAES $ClONO_2$

12 Feb | 1 Mar | 16 Mar

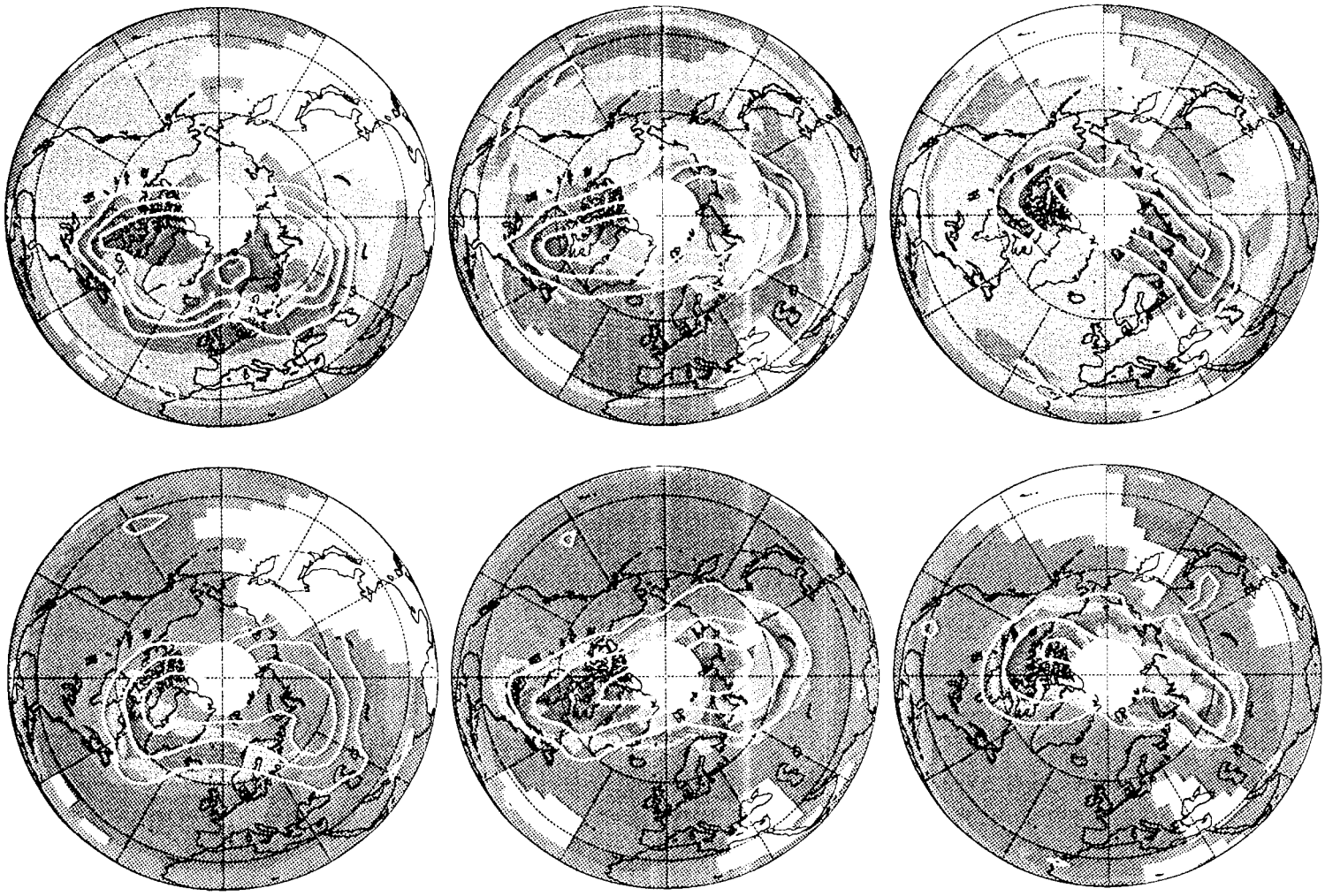

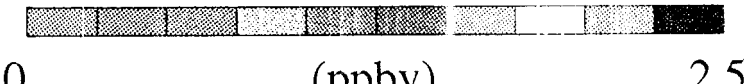

0. (ppbv) 2.5

Figure 14

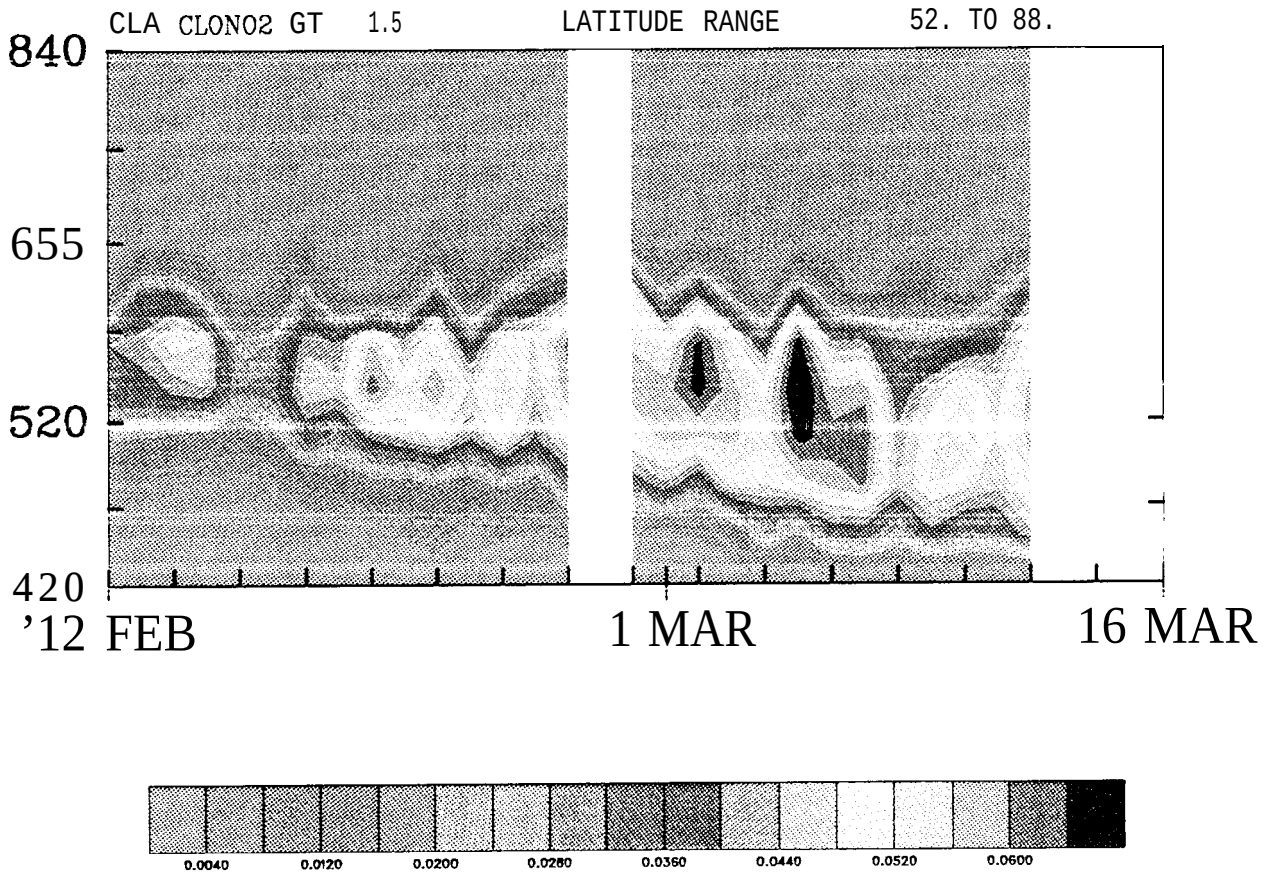
CLA CLONO2 GT 1.5
LATITUDE RANGE 52. TO 88.
840
655
520
420
'12 FEB
1 MAR
16 MAR
0.0040
0.0120
0.0200
0.0280
0.0360
0.0440
0.0520
0.0600

Figure 15

585 K
pv=1.050

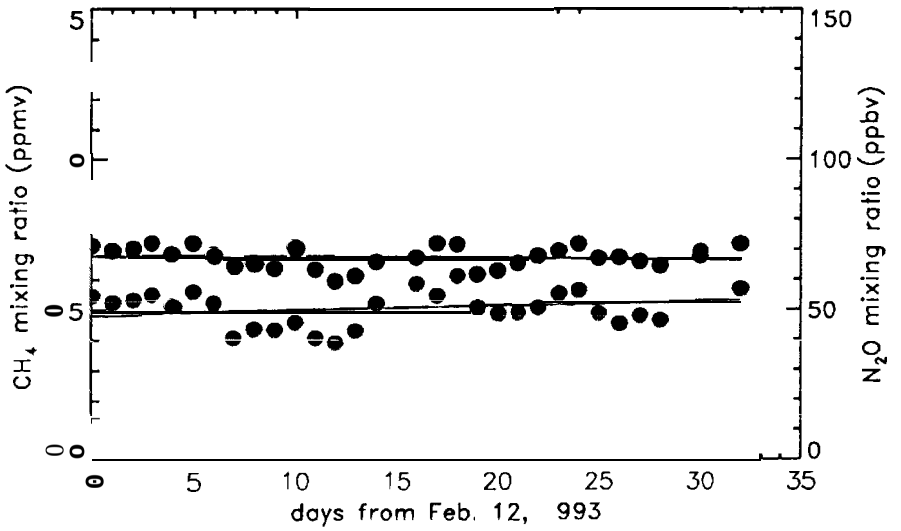

465 K
pv=0.375

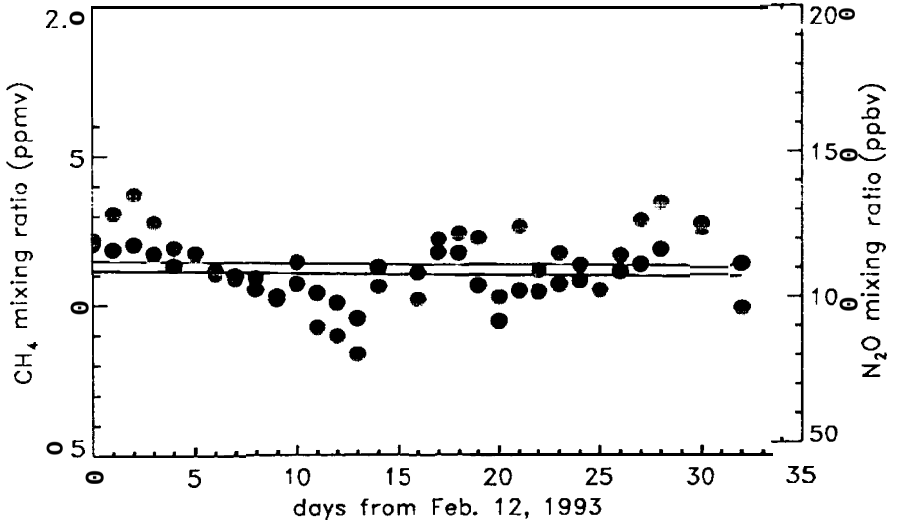

FIGURE 6

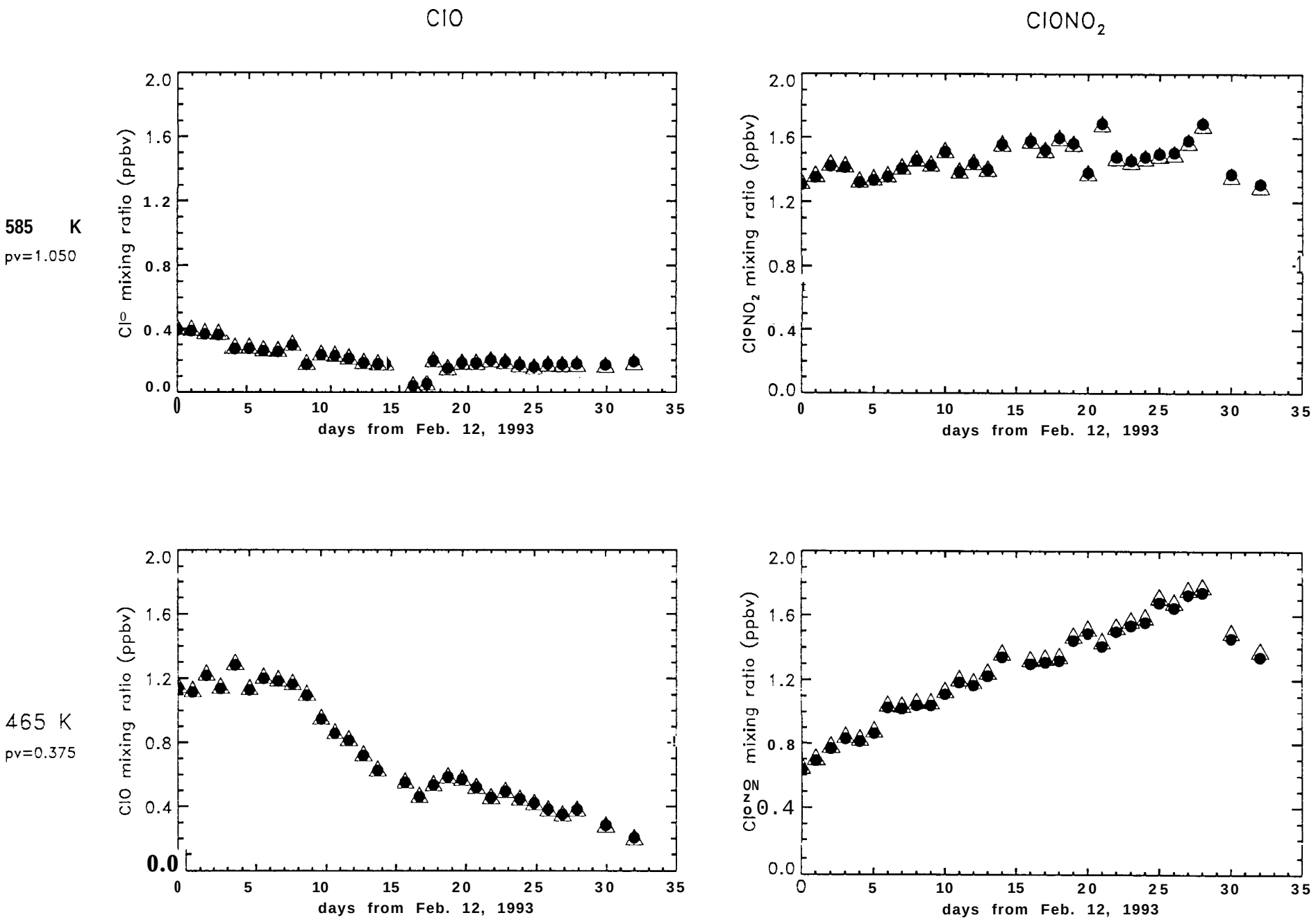
ClO
ClONO2
585 K
pv=1.050
465 K
pv=0.375
ClO mixing ratio (ppbv)
ClONO2 mixing ratio (ppbv)
days from Feb. 12, 1993
0.0
0.4
0.8
1.2
1.6
2.0
0
5
10
15
20
25
30
35

FIGURE 17

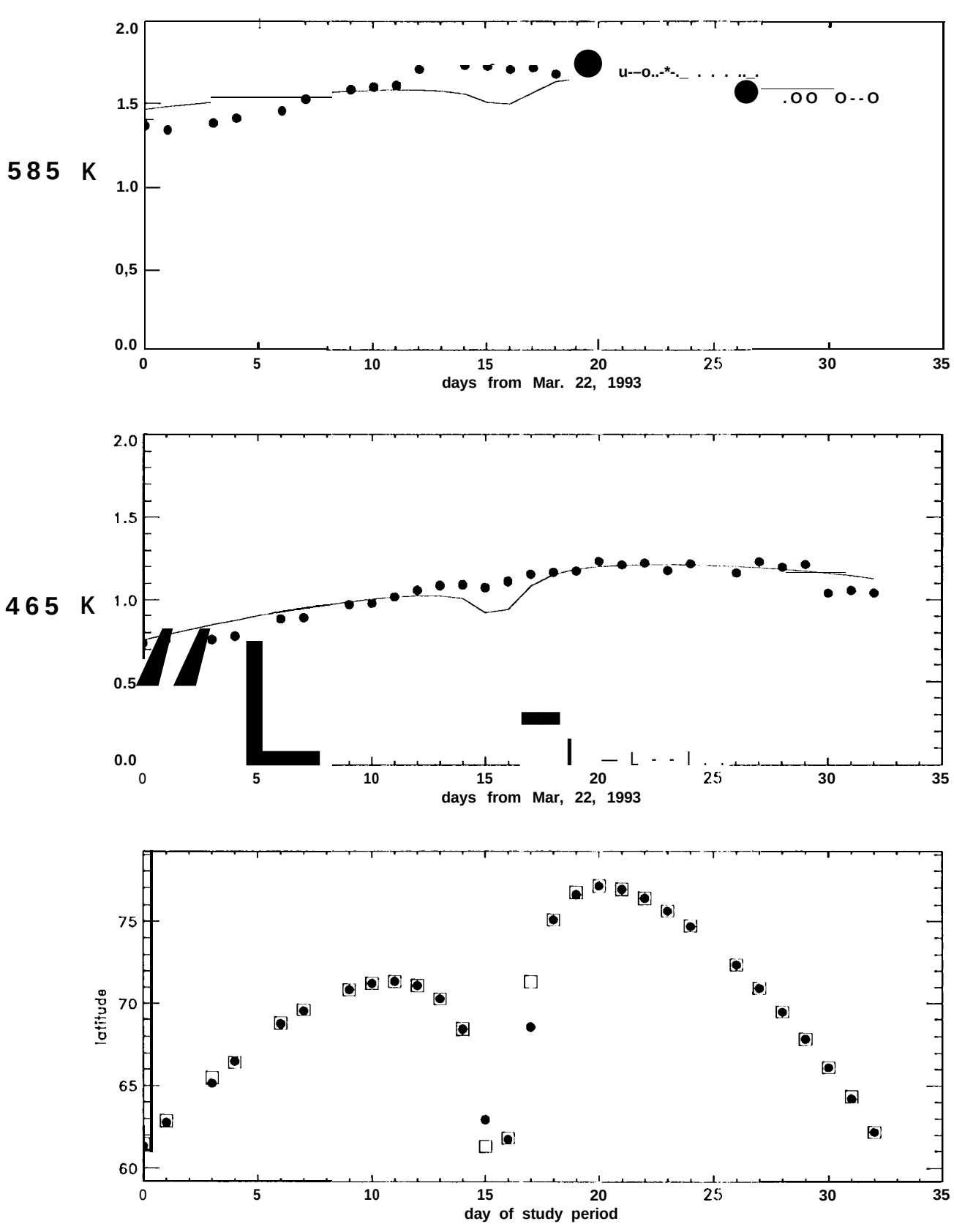
Daily--averaged I-ICl inside vortex
585 K
2.0
1.5
1.0
0,5
0.0
0
5
10
15
20
25
30
35
days from Mar. 22, 1993
465 K
2.0
1.5
1.0
0.5
0.0
days from Mar, 22, 1993
latitude
75
70
65
60
day of study period

Figure 18

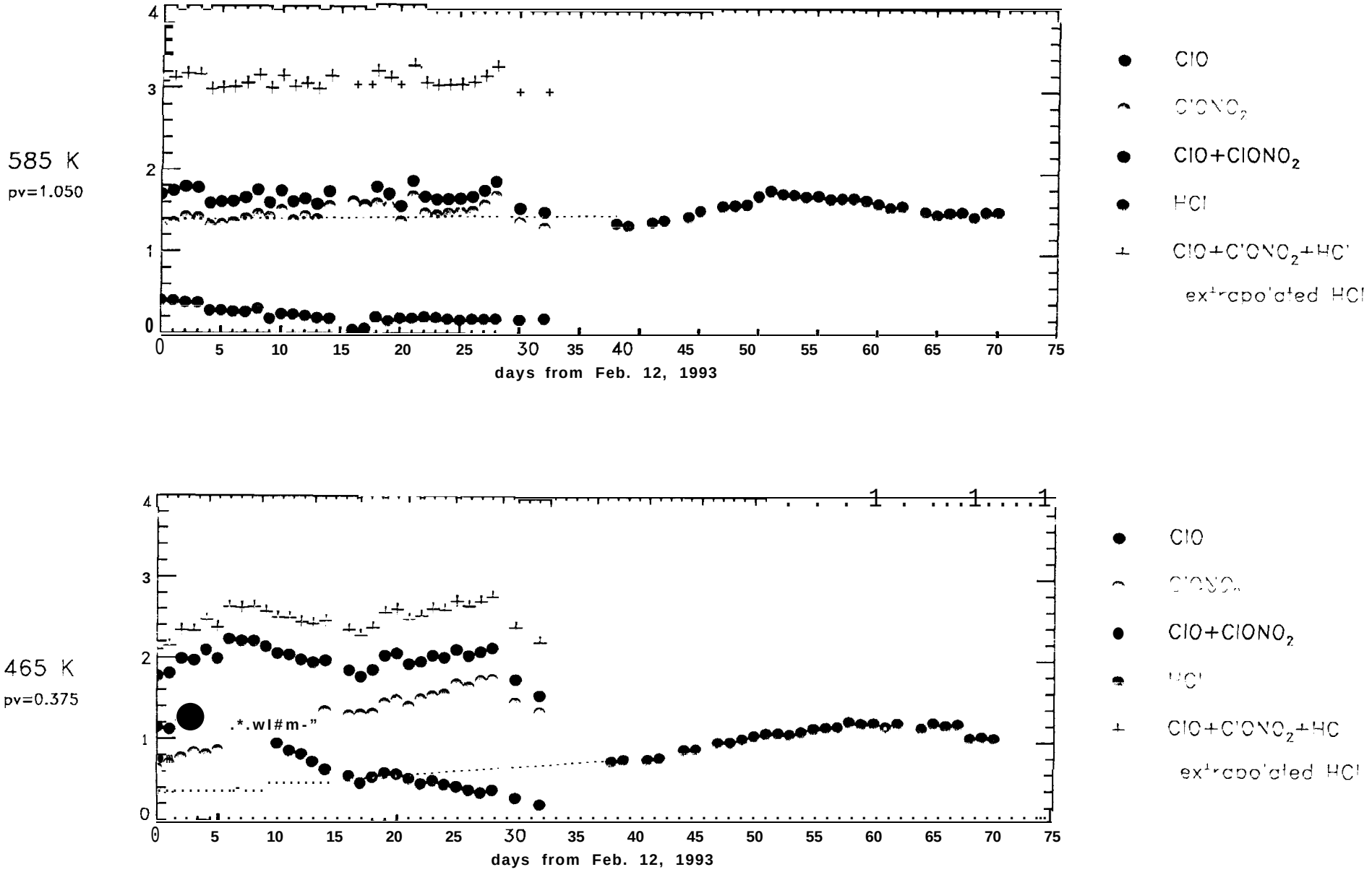
585 K
pv=1.050
ClO
ClONO2
ClO+ClONO2
HCl
ClO+ClONO2+HCl
extrapolated HCl
days from Feb. 12, 1993
465 K
pv=0.375
ClO
ClONO2
ClO+ClONO2
HCl
ClO+ClONO2+HCl
extrapolated HCl
days from Feb. 12, 1993

Figure 19